CDF/ANAL/EXOTIC/CDFR/xxxx
Version 0.1
December 11, 2007

Search for the Standard Model Higgs Boson Production in Association with $W^{\pm}$ Boson at CDF with $\int \mathcal{L}dt$ = 1.9 fb^{-1}

Jay Dittmann[1], Martin Frank[1], Richard Hughes[2], Shinhong Kim[6], Nils Krumnack[1], Kevin Lannon[2], Tatsuya Masubuchi[6], Yoshikazu Nagai[6], Jason Nielsen[5], Jason Slaunwhite[2], Anyes Taffard[3], Brian Winer[2], Weiming Yao[4]
[1]*Baylor University*
[2]*Ohio State University*
[3]*UC Irvine*
[4]*LBNL*
[5]*UC Santa Cruz*
[6]*University of Tsukuba*

Abstract

We present a search for Standard Model Higgs boson production in association with a $W^{\pm}$ boson. This search uses data through period 12, corresponding to an integrated luminosity of 1.9fb^{-1}. We select at least one tagged $W + 2$ jet events that fall into one of three tag categories: Events with two tight SECVTX tags or events with one tight SECVTX tag plus one jet probability tag or one tight SECVTX tag. Furthermore neural network b-tagging algorithm is applied to one SECVTX tag evens to improve signal-background ratio. Discrimination between the Higgs signal and the large backgrounds in the $W + 2$ jet bin is increased through the use of an artificial neural net. We see no evidence for a Higgs signal, so we set a 95% confidence level upper limit on the WH cross section times the branching ratio of the Higgs to decay to a $b\bar{b}$ pair. Using neural network discriminant gives best results

$$\sigma(p\bar{p} \to W^{\pm}H) \times BR(H \to b\bar{b}) < 1.3 \text{ to } 1.2 \text{ pb},$$

for Higgs masses from 110 GeV/c^2 to 150 GeV/c^2

1 Introduction

This note describes the search for $p\bar{p} \to WH \to \ell\nu b\bar{b}$ in events that are at least one b-tagged using the SECVTX and jet probability algorithms. The signature for this process is a W-boson decaying semileptonically to a high-p_T electron or muon and two jets containing

b-quarks (see Figure 1). This signature is primarily sensitive for low Higgs masses, as shown in Figure 2. The main backgrounds for this process include $W + 2$ jet production (where the jets contain either tagged heavy flavor or mistagged light flavor), $t\bar{t}$ production, and QCD multijet production, where one jet fakes a lepton. These background processes are essentially the same as the backgrounds for the $t\bar{t}$ search in the $W+ \geq 3$ jet bin, although in the case of $t\bar{t}$ the ratio of signal to background is much higher. This search uses data collected up to May 2007, which correspond to a total integrated luminosity of 1.9fb^{-1}.

The previous WH search [4] was performed with integrated luminosity of 1.7fb^{-1} and set an upper limit on the production cross section as shown in Figure 3. These limits ranged from $\sigma(WH) \times BR(H \rightarrow b\bar{b}) < 1.4$ pb for a Higgs mass of 110 GeV/c^2 to 1.1 pb for a Higgs mass of 150 GeV/c^2. For this version of the analysis, we take the following steps to improve the sensitivity:

1. We add one SECVTX tagged category to increase signal acceptance. The one SECVTX tagged events are applied to decrease background contamination

2. We improve an artificial neural network (NN) used in previous analysis to increase sensitivity.

We have investigated a number of other improvements, including adding additional acceptance through using PHX electrons and leptons identified as isolated tracks, and increasing the signal discrimination using more complicated multivariate techniques. We expect these improvements to be incorporated in the next update.

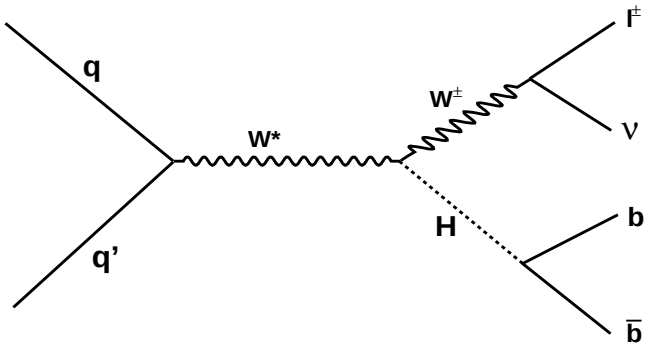

Figure 1: Feynman diagram of WH production.

2 Data/MC samples and Luminosity Calculation

The data used for this analysis come from the high p_T electron `bhel0d, bhel0h, bhel0i, bhel0j` and muon `bhmu0d, bhmu0h, bhmu0i, bhmu0j` datasets collected through

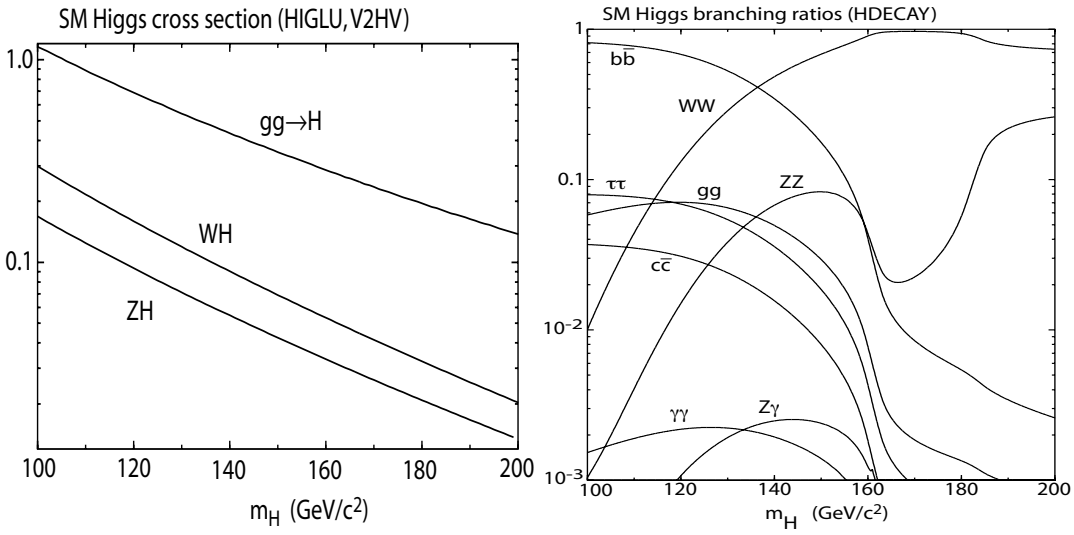

Figure 2: Standard model Higgs boson production cross section at the Tevatron and the branching ratio of Higgs boson.

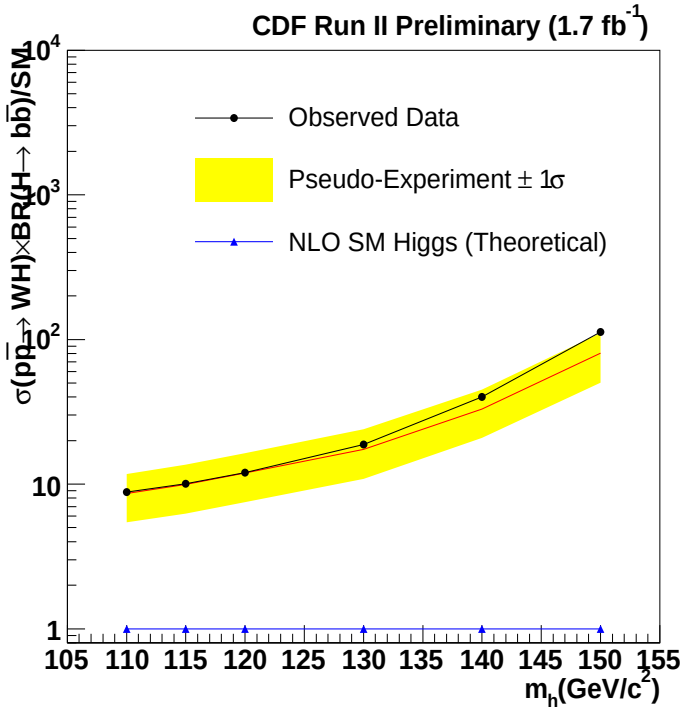

Figure 3: Upper limit on $\sigma(p\bar{p} \to WH) \times BR(H \to b\bar{b})$ obtained with integrated luminosity of $955pb^{-1}$.

March 2007. We select events from these datasets that pass the central electron (ELECTRON_CENTRAL_18) and central muon (MUON_CMUP18 and MUON_CMX18) triggers. Due to trigger bandwidth limitations at high luminosity, several versions of the muon trigger: a luminosity-enabled version, which disables the CMX trigger until a certain luminosity is reached, a "JET10" version, which adds an additional jet requirement, and at the highest luminosities, one that combines the luminosity enable and jet requirement. The luminosity lost to the luminosity enabled CMX triggers is accounted for when the sample luminosity is calculated. Luminosities are calculated using the DQM version 18 good run list (bits [1,1,4,1]). The corresponding total integrated luminosity is $1.92\,\mathrm{fb}^{-1}$ for CEM and CMUP leptons, $1.88\,\mathrm{fb}^{-1}$ for CMX muons.

Our Higgs signal model comes from the official Higgs Discovery Group Higgs Monte Carlo (MC) samples generated with PYTHIA using the standard MC procedure outlined in CDF software version 6.1.4. These Higgs samples were generated for a range of Higgs masses (M_h = 110, 115, 120, 130, 140 and 150 GeV). Our background models are composed of a number of components. The W and Z plus light flavor and heavy flavor jet processes are modeled using ALPGEN version 2.10 showered with PYTHIA. Likewise, the single-top contribution is modeled using parton-level events generated by MadEvent and showered through PYTHIA. The rest of the background processes, including the $t\bar{t}$, WW, WZ, and ZZ processes were generated with PYTHIA. For backgrounds involving a top quark, the top mass was set to 175 GeV/c^2.

3 Event Selection

We use the same event selection criteria as in the SECVTX $t\bar{t}$ cross section measurement [14]. We require events to contain an isolated electron or muon with $E_T(p_T) > 20$ GeV as well as $\not\!\!E_T > 20$ GeV, after accounting for the muon and jet energy corrections. Jets are clustered using JETCLU with a cone size of 0.4 and are required to have $E_T > 20$ GeV after level 5 jet corrections (using `jetCorr12` jet energy correction code) and $|\eta_{Detector}| < 2.0$. Currently, we are not using any additional QCD veto, such as the standard cut on the angle between the $\not\!\!E_T$ and the leading jet. The tagged sample is defined by requiring that at least one of the jets has a positive tight SECVTX tag.

3.1 b-tagging strategies

In the previous version of this analysis, we focused double b-tagging events which have double SECVTX tagged events or one SECVTX tag plus one Jet Probablity tagged events. For this version of the analysis, we try to include the single SECVTX tagged events. Because these events still have large signal acceptance. However the background contamination is much worse than double tagged events. Therefore, we apply NN flavor separation [5] for one tagged events. Finally, events used in this search fall into one of three exclusive categories:

SECVTX tight + SECVTX tight (ST+ST): Events in this category are required to have both jets tagged by the tight operating point of SECVTX.

SECVTX tight + Jet Probability (ST+JP): Events in this category are required to have one jet tagged by the tight operating point of SECVTX and one jet to be tagged by the jet probability algorithm. To be tagged, a jet must have a jet probability of less than 5%.

SECVTX tight w/ NN tag: Events in this category are required to have exact one SECVTX tight tagged jet and its jets need to pass NN separator.

Figure 4 shows comparison between the b-tagging categories used in this version of the analysis and the previous version. Almost all tagging events of at least one SECVTX agged events is utilized in this analysis.

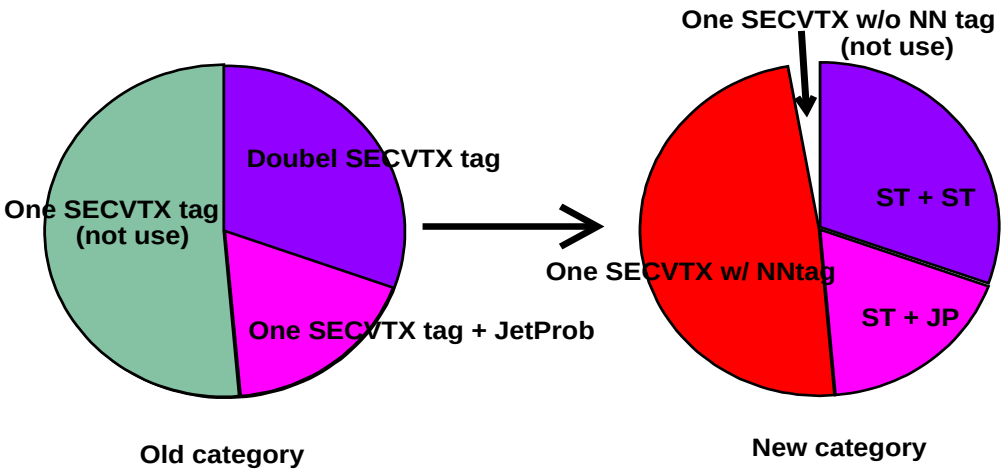

Figure 4: b-tagging category comparison between the current analysis and the previous one. Left plot shows b-tagging category in previous analysis and right plot show b-tagging category in this analysis

4 Background Estimation

In this note, we build on the method of background estimation used in $t\bar{t}$ cross section measurement[14], the so-called "Method 2". In the W+jets sample, the following background sources are considered:

Non-W QCD: A W signature is generated when one jet fakes a high p_T lepton and $\not\!\!E_T$ is generated through jet energy mismeasurement.

W + Mistags: This background occurs when one or more light flavor jets produced in association with a W boson are mistakenly identified as a heavy flavor jet by the b-tagging

algorithms. Mistags are generated because of the finite resolution of the tracking, because of material interactions, or because of long-lived light flavor hadrons (Λ and K_s) that produce displaced vertices.

W+ Heavy Flavor: These processes ($W + b\bar{b}$, $W + c\bar{c}$ and $W + c$) involve the production of actual heavy flavor quarks in association with a W boson.

Top Quark Backgrounds: This background comes both from single top quark production and top quark pair production.

Other EWK Backgrounds: Additional small background contributions come from Z + jets production and diboson (WW, WZ, and ZZ) production.

The Non-W background is estimated using the "MET vs ISO" technique described below. The W + Mistag background is estimated from the data by apply a mistag parameterization, also known as the mistag matrix, to the data before tagging (pretag data). The W + Heavy Flavor background is also estimated from the pretag data using the ALPGEN + PYTHIA MC to set the relative normalization of light to heavy flavor events as well as the b-tagging efficiency for W + Heavy Flavor events (see below). The Top Quark and Other EWK backgrounds are normalized directly by their theoretical cross sections, calculated at next-to-leading order. More details can be found in the $t\bar{t}$ cross section documentation [14].

4.1 NonW (QCD fake) background

To estimate the number of events in which QCD jets fakes a lepton, we use the $\not\!\!E_T$ vs Isolation method. We divide the $\not\!\!E_T$ vs isolation plane into the following regions (see Figure 5):

- region A: Isolation $>$ 0.2 and $\not\!\!E_T < 15$ GeV
- region B: Isolation $<$ 0.1 and $\not\!\!E_T < 15$ GeV
- region C: Isolation $>$ 0.2 and $\not\!\!E_T > 20$ GeV
- region D: Isolation $<$ 0,1 and $\not\!\!E_T > 20$ GeV

Here region D is our signal region. We assume that the lepton isolation is independent of $\not\!\!E_T$, and that the tagging efficiency is the same between Region B and D. Then we define the fraction of events which are the non-W contribution:

$$f_{\text{non}-W} = \frac{N_B \times N_C}{N_A \times N_D}, \tag{1}$$

where N_i $(i = A, B, C, D)$ are the number of pretag events in each sideband region. To obtain the non-W background for tagged events, we measure the b-tagging efficiency from region B. For this purpose, we define tagging efficiency as

$$r_B = \frac{N_B^{(\text{tagged events})}}{N_B^{(\text{taggable jets})}}, \tag{2}$$

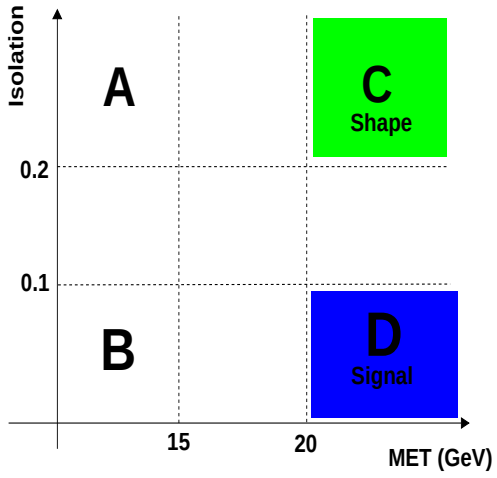

Figure 5: Each region in $\not\!\!E_T$ and L lepton isolation plane

where $N_B^{(\text{tagged jets})}$ and $N_B^{(\text{taggable jets})}$ are number of taggable and tagged jets in region B respectively. Then we obtain the non-W background in region D with the relation

$$N_D^{(\text{non}-W)} = f_{\text{non}-W} \times r_B \times N_D^{(\text{taggable jets})}. \tag{3}$$

We call this procedure the "Tag Rate Method" since it uses the tag rate in region B. It is also possible to have a estimate directly from the tagged sample, by using

$$N_D^+ = \frac{N_B^+ \times N_C^+}{N_A^+}, \tag{4}$$

where $+$ denotes positive tagged events, and we call this method as "Tagged Method" in this note.

These methods are data-based techniques, so the estimates could also contain other background processes. Subtracting the known backgrounds should result in a better non-W QCD estimate. The contributions from $t\bar{t}$ and W+jets events to each sideband region are estimated and subtracted based on theoretical cross section and ratio to D region. The non-W fractions after the correction are shown in Table 1. Systematic uncertainty of nonW fraction ,25%, are quoted from previous analysis[3] as there are no reason from previous.

To combine the estimates from the tag rate and tagged methods, the two sums are combined in a weighted average to get the total non-W backgrounds.

The low statistics of the double-tagged and NN tagged samples prevents us from applying this technique directly. Instead, estimates from the $\geq$ 1-tagged sample are extended into the double-tagged or NN tagged sample using the ratio of at events with at least 1 tag to events with double tag events in region A'(Isolation > 0.1 and $10 < \not\!\!E_T < 20$ GeV), B, and C'(Isolation > 0.1 and $\not\!\!E_T > 20$ GeV).

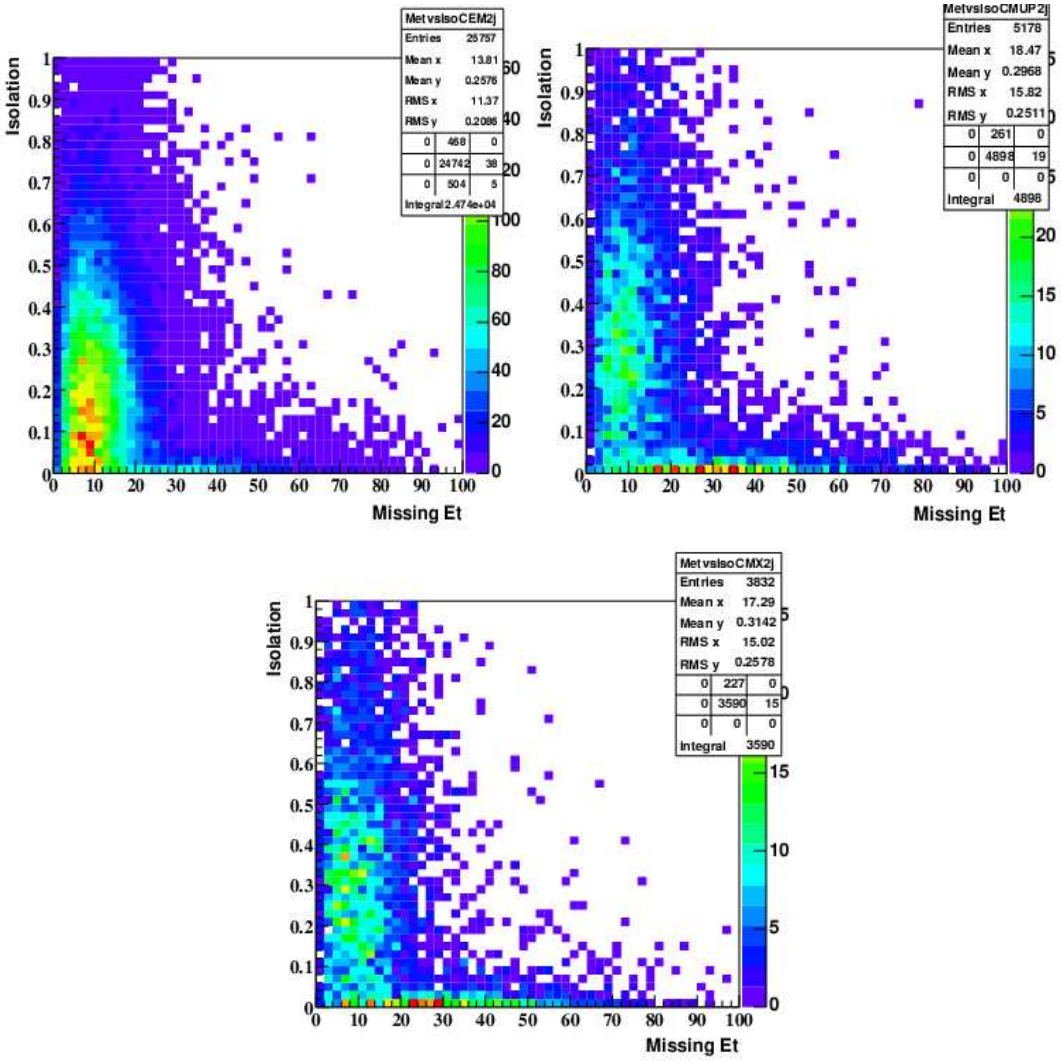

Figure 6: Observed data on $\not\!\!E_T$ vs Iso plane. From left, CEM, CMUP and CMX region. These events has exact 2 tight jets

4.2 W + Heavy flavor

The $Wb\bar{b}$ and $Wc\bar{c}$ states are major sources of background of b-tags in the W+jets channel. They are estimated primarily from the Monte Carlo, but their overall rates are normalized to data. The contribution from true heavy flavor production in W+jet events is determined from measurements of the heavy flavor event fraction in W+jet events and the tagging efficiency for those events.

These heavy flavor fractions and a scaling factor for these fractions (k-factor) have been studied extensively elsewhere [15, 14] using ALPGEN v2 + PYTHIA Monte Carlo. Heavy flavor fractions measured in ALPGEN have been calibrated using a jet data sample, and it is found that a k-factor of 1.4 ± 0.4 is necessary to make the heavy flavor production in

Njets	1jet	2 jet	>= 3jet
bhel0d	0.209±0.052	0.232±0.059	0.248±0.065
bhmu0d	0.055±0.014	0.071±0.018	0.090±0.025
bhel0h	0.236±0.059	0.251±0.063	0.251±0.065
bhmu0h	0.056±0.014	0.067±0.017	0.058±0.016
bhel0i	0.246±0.062	0.260±0.066	0.215±0.057
bhmu0i	0.054±0.014	0.071±0.018	0.073±0.021
bhelmi (Period 8)	0.257±0.065	0.264±0.067	0.280±0.075
bhmumi (Period 8)	0.054±0.014	0.072±0.019	0.078±0.023
bhelmi2 (Period 9)	0.258±0.065	0.291±0.074	0.256±0.069
bhmumi2 (Period 9)	0.057±0.014	0.065±0.017	0.061±0.019
bhelmi3 (Period 10)	0.275±0.069	0.277±0.070	0.308±0.081
bhmumi3 (Period 10)	0.059±0.015	0.073± 0.019	0.038±0.011
bhel0j (Period 11)	0.287±0.072	0.285± 0.072	0.84±0.075
bhmu0j (Period 11)	0.055±0.014	0.080±0.021	0.068±0.020
bhelmj2 (Period 12)	0.279±0.07	0.287± 0.073	0.285±0.077
bhmumj2 (Period 12)	0.059±0.015	0.075±0.020	0.068±0.021

Table 1: NonW fraction after correction for each dataset and each jet bin. 3 jet and more than 3 jet is merged due to statistical limitation

One SECVTX w/ NN tag	1jet	2 jet	3 jet	>=4 jet
WBB (1B)	27.5±1.49	28.1±1.25	26.7±1.42	26.9± 3.67
WBB (2B)		26.2±1.22	24.1±1.23	22.6±1.31
WCC (1C)	4.17±0.23	4.59±0.25	4.91±0.29	5.23±0.66
WCC (2C)		6.28±0.38	6.56±0.42	6.85±0.64

Table 2: Heavy flavor tagging efficiency calculated from ALPGEN v2 W+jets MC for one SECVTX w/ NNtag category.

Monte Carlo match the production in data. Although we can apply most of the numbers from Ref [14] without modification, we need to calculate the tagging efficiency of the ST+JP and one SECVTX tag w/ NNtag categories ourselves. Table 2,3 show the heavy flavor tagging efficiency results for these two categories. The heavy flavor fractions and tagging efficiencies are multiplied by the number of pre-tagged events in data, after the number of pre-tagged events has been corrected for the non-W and other background contribution.

$$N_{W+HF} = f_{HF} \cdot \epsilon_{\rm tag} \cdot [N_{\rm pretag} \cdot (1 - f_{\rm non-W}) - N_{\rm EWK}], \quad (5)$$

where f_{HF} is heavy fraction, $\epsilon_{\rm tag}$ is tagging efficiency and $N_{\rm EWK}$ is the expected number of $t\bar{t}$ and diboson events.

SECVTX + Jet Probability(5%)	2 jet	3 jet	>=4 jet
WBB (2B)	10.1±1.2	11.1±1.3	12.4±1.5
WCC (2C)	1.6±0.2	2.3±0.3	3.2±0.4

Table 3: Heavy flavor tagging efficiency calculated from ALPGEN v2 W+jets MC for double b-tagging categories.

4.3 Mistag

The rate of W + mistag, or falsely tagged, jets is derived from a sample of events collected with a jet-based trigger with no heavy flavor requirement. The mistag rate is obtained using negative tags, which are tags that appear to travel back toward the primary vertex. The mistag rate obtained from negative tags is parameterized in bins of η, jet E_T, track multiplicity within a jet, $\sum E_T$ of the event, number of z vertices, and the z vertex position [12]. The mistag rate derived from negative tags is corrected for the effects of heavy flavor in the jet sample, long-lived light flavor vertices, and vertices caused by material interactions in the silicon detector. This correction is parameterized as a function of E_T to reduce its systematic uncertainty [13].

Tag rate probabilities for events with at least one SECVTX tag are obtained by summing over all of the taggable jets in pretag events and exact one tag events. For double tagged events, we apply a similar procedure to events with exactly one tight SECVTX tag, summing tag rate probabilities for all taggable jets except the tagged one. The total mistag normalization is obtained by adding up all the mistag probability event sums for the pretag events. Figure 7 illustrates our mistag background calculation scheme.

The uncertainty on the mistag estimate includes the statistical errors from the matrix itself, accounting for correlations between jets which fall in the same bin of the mistag matrices, and an additional 5.9% error from all systematic uncertainties [12]. Although the mistag matrix was derived using the 1.12fb^{-1} sample, it has been shown that it is acceptable to apply this at least through period 10 data as long as the systematic uncertainties are increased by 1.8% to cover possible discrepancies.

For jet probability, mistag matrix is applied like SECVTX tag. This matrix is parametrized in E_T ,η, ϕ of jet, Number of track, sumE_T , z vertex position.

For NN b-tagging, we apply rejection factor 0.35±0.05 to one SECVTX tagged events estimated in CDF note [5]

4.4 MC derived background

The normalization of the diboson, $t\bar{t}$ and single top backgrounds are based on the theoretical cross sections (listed in Table 4), the measured luminosity and the acceptance and b-tagging efficiency derived from MC. The MC acceptance is corrected for lepton identification, trigger efficiencies and z vertex cut. The tagging efficiency is always scaled by the MC/data scale factor of 0.95± 0.05 for SECVTX and 0.85±0.07 for jet probability. For NN b-tag, the

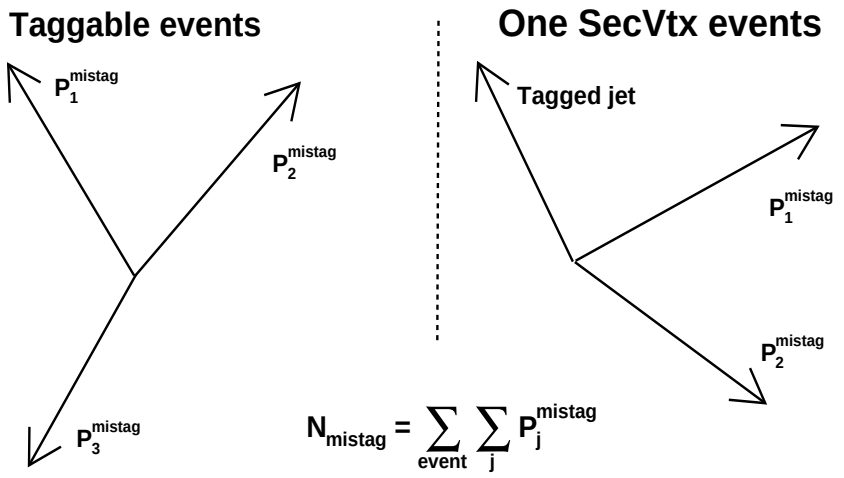

Figure 7: Mistag calculation in each tag

Theoretical Cross Sections	
WW	12.4 $\pm$ 0.25 pb
WZ	3.96 $\pm$ 0.06 pb
ZZ	1.58 $\pm$ 0.05 pb
Single Top s-channel	0.88 $\pm$ 0.11 pb
Single Top t-channel	1.98 $\pm$ 0.25 pb
$Z \to \tau\tau$	265 $\pm$ 30.0 pb
$t\bar{t}$	6.7 $^{+0.7}_{-0.9}$ pb

Table 4: Theoretical cross sections and errors for the electroweak and single top backgrounds, along with the theoretical cross section for $t\bar{t}$ at ($m_t = 175$GeV/c^2). The cross section of $Z^0 \to \tau\tau$ is obtained from direct CDF measurement.

tagging efficiency is scaled by the factor 0.97$\pm$0.02. The expected number of events is obtained by the equation

$$N = \int \mathcal{L}dt \times \epsilon \times \sigma, \tag{6}$$

where ϵ is the total detection efficiency corrected by all of the scale factors.

4.5 Background summary

We have described the contributions of individual background sources to the final background estimate. The summary table of the background estimates are shown in Tables.5-**??**

and number of expected events and observed data as a function of jet multiplicity plots are shown in Figure **??-??**

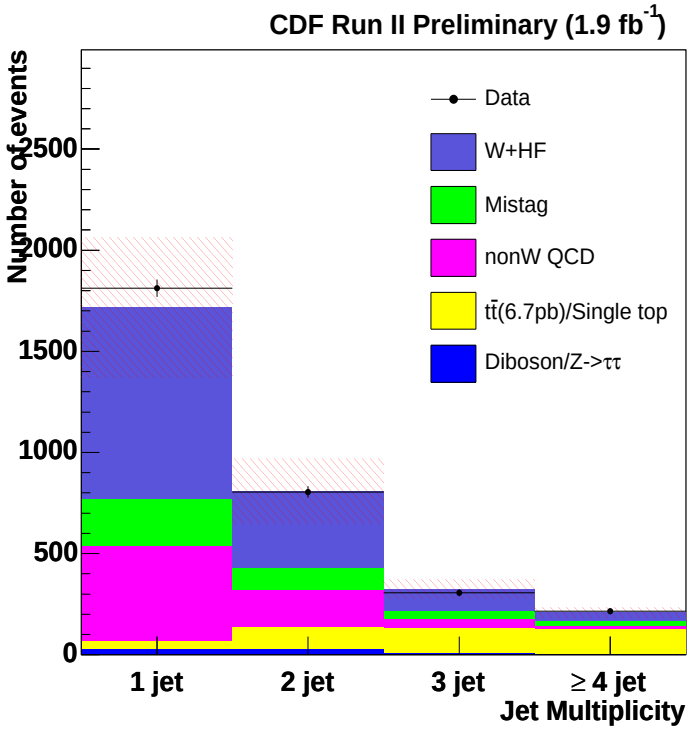

Figure 8: The number of observed one SECVTX tag w/ NN tagged events and background estimation summary as a function of jet multiplicity. Black points show observed events and each color means each estimated background. Red hash means background uncertainties.

Njet	1jet	2jet	3jet	>=4jet
Pretag Events	196160	32242	5496 1494	
Mistag	236.7±19.36	107.1±9.38	41.84±3.839	20.97±1.91
$Wb\bar{b}$	431.7±182.4	215.6±92.34	61.78±24.68	26.14±10.43
$Wc\bar{c}$	514.4±154.7	167±62.14	45.4±15.31	17.71±6.86
$t\bar{t}$(6.7pb)	11.85±1.82	60.68±9.30	111±17.03	122.4±18.76
Single top(s-ch)	7.09±1.03	14.38±2.09	3.91±0.57	0.97±0.14
Single top(t-ch)	23.31±3.41	29.57±4.33	6.24±0.91	1.11±0.16
WW	7.21±0.89	15.45±1.91	4.61±0.57	1.03±0.13
WZ	5.52±0.59	7.59±0.81	1.76±0.19	0.48±0.05
ZZ	0.17±0.02	0.31±0.03	0.14±0.01	0.07±0.01
$Z->\tau\tau$	14.58±2.25	7.27±1.12	2.39±0.37	0.71±0.11
nonW QCD	465±83.21	184.7±33.04	44.83±8.57	17.03±3.67
Total Bkg	1717.6±347.89	809.61±159.38	323.92±45.45	208.57±26.24
WH signal (120 GeV)	Control region	1.82±0.15	Control region	Contral region
Observed Events	1812	805	306	215

Table 5: Background summary table for one tag w/ NNtag category

Njet	2jet	3jet	>=4jet
Pretag Events	32242	5496	1494
Mistag	3.88±0.35	2.41±0.24	1.62± 0.14
$Wb\bar{b}$	37.93±16.92	14.05±5.49	7.39± 2.93
$Wc\bar{c}$	2.88±1.25	1.52±0.61	1.15± 0.47
$t\bar{t}$(6.7pb)	19.05±2.92	54.67±8.38	94.93± 14.56
Single top(s-ch)	6.90±1.00	2.28±0.33	0.61± 0.088
Single top(t-ch)	1.60±0.23	1.43±0.21	0.50± 0.07
WW	0.17±0.02	0.15±0.02	0.16± 0.02
WZ	2.41±0.26	0.68±0.07	0.16± 0.02
ZZ	0.06±0.01	0.06±0.01	0.02±0.001
$Z->\tau\tau$	0.25±0.04	0.19±0.03	0.06±0.01
nonW QCD	5.50±1.00	2.56±0.48	1.02± 0.22
Total Bkg	80.62±18.75	79.99±10.92	107.63± 15.15
WH signal (120 GeV)	0.94±0.11	Control region	Control region
Observed Events	83	88	118

Table 6: Background summary table for double SECVTX tag category

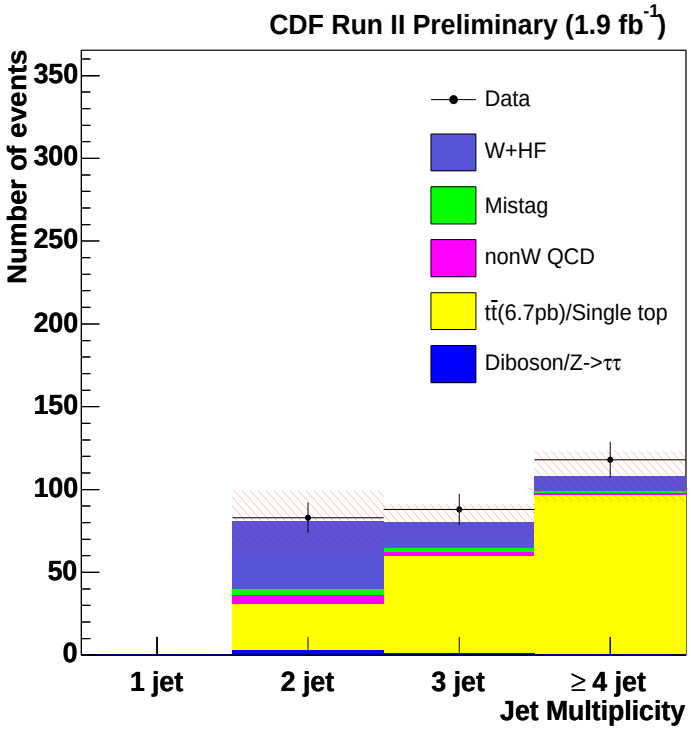

Figure 9: The number of observed double SECVTX tagged events and background estimation summary as a function of jet multiplicity. Black points show observed events and each color means each estimated background. Red hash means background uncertainties.

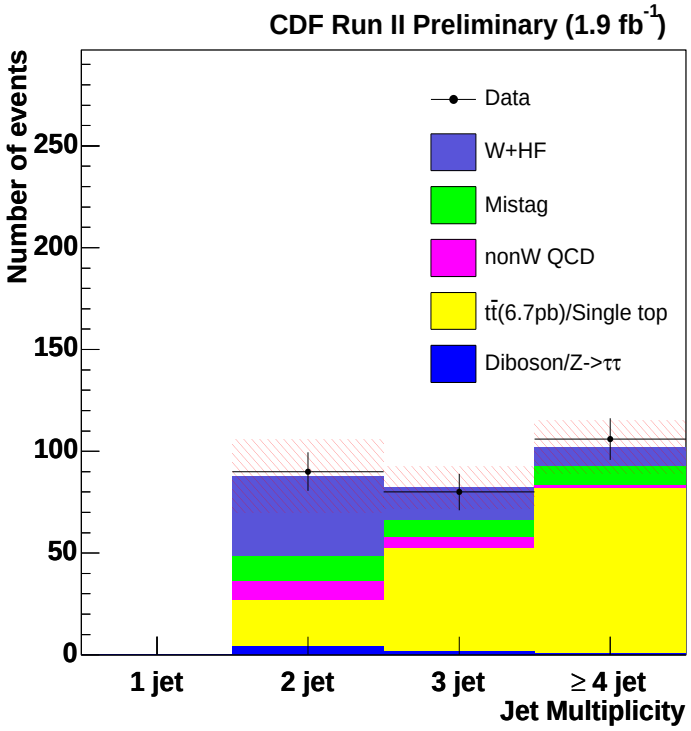

Figure 10: The number of observed one SECVTX and one Jet probability tagged events and background estimation summary as a function of jet multiplicity. Black points show observed events and each color means each estimated background. Red hash means background uncertainties.

Njet	2jet	3jet	>=4jet
Pretag Events	32242	5496	1494
Mistag	12.51±0.98	8.69±0.69	8.99±0.63
$Wb\bar{b}$	31.15±14.03	11.47±4.55	6.55±2.63
$Wc\bar{c}$	7.87±3.43	4.38±1.76	3.09±1.27
$t\bar{t}$(6.7pb)	15.56±2.39	47.48±7.28	79.81±12.24
Single top(s-ch)	5.14±0.75	1.90±0.27	0.53±0.07
Single top(t-ch)	1.87±0.27	1.49±0.22	0.44±0.06
WW	0.93±0.11	0.63±0.08	0.47±0.06
WZ	1.84±0.20	0.59±0.06	0.19±0.02
ZZ	0.08±0.01	0.04±0.003	0.02±0.002
$Z->\tau\tau$	1.29±0.20	0.53±0.08	0.20±0.03
nonW QCD	9.55±1.73	4.87±0.93	1.80±0.40
Total Bkg	87.77±17.99	82.04±10.22	102.09±13.09
WH signal (120 GeV)	0.74±0.09	Control region	Control region
Observed Events	90	80	106

Table 7: Background summary table for one SECVTX tag + Jet Probability tag category

5 Higgs Signal Acceptance

5.1 Introduction

To calculate the expected number of signal $N_{WH\to l\nu b\bar{b}}$, the following equation is used:

$$N_{WH\to l\nu b\bar{b}} = \epsilon_{WH\to l\nu b\bar{b}} \cdot \mathcal{L} \cdot \sigma(p\bar{p} \to WH) \cdot Br(H \to b\bar{b}), \tag{7}$$

where, $\epsilon_{H\to l\nu b\bar{b}}$ is detection efficiency for signal, $\mathcal{L}$ is the integrated luminosity, $\sigma(p\bar{p} \to WH)$ is WH production cross section in proton antiproton collisions and $BR(H \to b\bar{b})$ is branching ratio for Higgs decaying to $b\bar{b}$. The detection efficiency for signal events is defined as:

$$\epsilon_{WH\to l\nu b\bar{b}} = \epsilon_{Z0} \cdot \epsilon_{trig} \cdot \epsilon_{leptonid} \cdot \epsilon^{MC}_{WH\to l\nu b\bar{b}} \cdot \left(\sum_{l'=e,\mu,\tau} BR(W \to l'\nu) \right), \tag{8}$$

where $\epsilon^{MC}_{WH\to l\nu b\bar{b}}$ is the fraction of signal events (with $|z_0| < 60$cm) which pass the kinematic and b-tagging requirements. The effect of the b-tagging scale factor in this fraction is included by randomly selecting tagged jets to discard. The quantity ϵ_{Z0} is efficiency of the $|z_0| < 60$ cm cut, and is measured in data. The trigger efficiencies for high p_T leptons, ϵ_{trig}, are also measured in data using back-up triggers with looser requirements [7, 9]. The lepton id and reconstruction efficiencies measured in Monte Carlo are corrected by scale factors, $\epsilon_{leptonid}$ derived from data [8, 9]. Finally, $Br(W \to l'\nu)$ is the branching ratio for leptonic (e, μ) W decay. Each of these factors and their systematic errors are treated separately for each data period and the results are combined weighted by the luminosity of each data period. For the later data periods, where numbers may not have been finalized, preliminary results have been taken from the slides of talks given in the Joint Physics meeting [10].

Samples of PYTHIA $WH \to l'\nu b\bar{b}$ Monte Carlo with Higgs boson masses of m_H = 110, 115, 120, 130, 140 and 150 GeV/c^2 are used to estimate $\epsilon^{MC}_{WH\to l\nu b\bar{b}}$. The run range of these MC samples covers up to period 8 run range, and we estimate the signal expectations for each period independently due to the different acceptances. As we don't have MC samples corresponding to period 9 or later, we assume that periods 9-12 acceptance is same as period 8 and scale up the contribution from period 8 to account for the luminosities in periods 9-12.

Finally, we combine the numbers from each run period, weighted by the appropriate luminosity, to obtain our final acceptance number. Figure 11 show the overall acceptance for each b-tagging condition including all systematic effects as a function of Higgs mass. The acceptance increases linearly from 0.91%$\pm$0.05 to 1.01%$\pm$0.06 as a function of Higgs mass for one SECVTX tight tag w/ NN tag. The acceptances for tight SECVTX double-tagged selection are from 0.42%$\pm$0.04 to 0.51%$\pm$0.05. For the tight SECVTX tag + jet probability category, the acceptance are from 0.36$\pm$0.04 to 0.43$\pm$0.05, even though these categories are exclusive sample to double SECVTX tag category. Table 8 shows the acceptance for a number of Higgs masses for the various tagging categories. Systematic uncertainties are discussed in detail in the following subsection.

The expected number of WH signal events is estimated from the calculated acceptance at each mass. The expectation for each event selection is shown in Tables 9. In these tables

b-tagging category	110 GeV	115 GeV	120 GeV	130 GeV	140 GeV	150 GeV
One tag w/ NNtag	0.91±0.05	0.93±0.05	0.93±0.05	0.97±0.05	1.01±0.06	1.01±0.06
ST + ST	0.42±0.04	0.44±0.05	0.48±0.05	0.51±0.05	0.51±0.05	0.51±0.05
ST + JP	0.36±0.04	0.38±0.04	0.38±0.04	0.42±0.04	0.43±0.05	0.43±0.05

Table 8: WH signal acceptance table in W+2jet events for each tag category and each mass samples. Systematic error is included in uncertainties. Each tagging category is exclusive to other categories

b-tagging category	110 GeV	115 GeV	120 GeV	130 GeV	140 GeV	150 GeV
One tag w/ NNtag	2.81±0.23	2.35±0.19	1.82±0.15	1.15±0.09	0.59±0.05	0.23±0.02
ST + ST	1.31±0.16	1.11±0.14	0.94±0.11	0.61±0.07	0.30±0.04	0.11±0.01
ST + JP	1.11±0.13	0.94±0.11	0.74±0.09	0.50±0.06	0.25±0.03	0.10±0.01

Table 9: WH signal expected table calculated with integrated luminosity 1.9 fb^{-1} in W+2jet events for each tag category and each mass samples. Systematic error is included in uncertainties. Each tagging category is exclusive to other categories

expected events are calculated from 2 jet bin only. The WH production cross section and branching ratio (Figure 2) on the Higgs Working Group page [1, 2] are used .

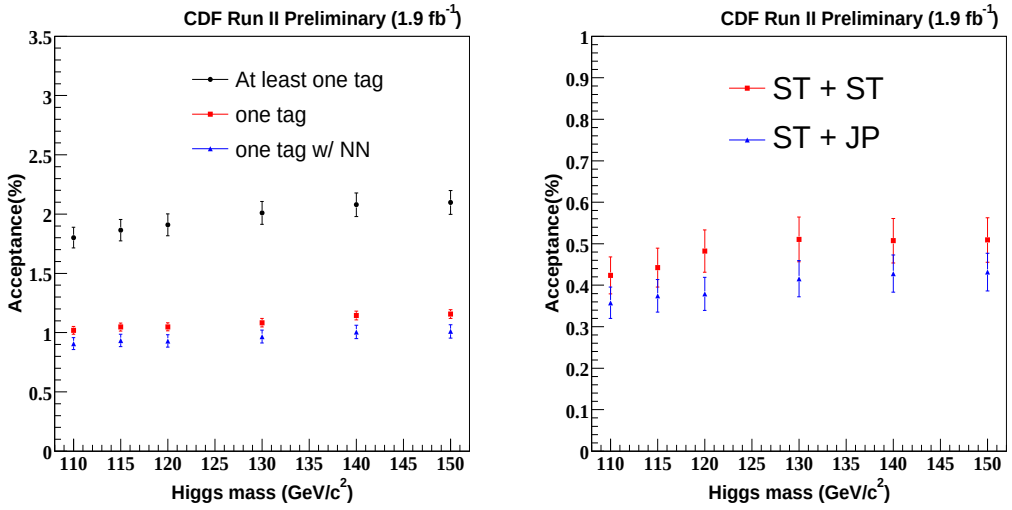

Figure 11: Signal acceptance as a function of Higgs mass. Left plot shows the at least one tag and exactly one tag category (w/ NN tag). Right plot shows the double tag categories.

b-tagging category	LeptonID	Trigger	ISR/FSR	JES	PDF	b-tagging	Total
One tag w/ NN tag	$\sim 2\%$	$< 1\%$	2.9%	2.3%	1.2%	3.5%	5.6%
ST + ST	$\sim 2\%$	$< 1\%$	5.2%	2.5%	2.1%	8.4%	10.6%
ST + JP	$\sim 2\%$	$< 1\%$	4.0%	2.8%	1.5%	8.9%	10.5%

Table 10: Systematic uncertainties for each tagging category

5.2 Systematic Uncertainties on Acceptance

The systematic uncertainties on the acceptance include uncertainties on the jet energy scale, initial and final state radiation, lepton ID and trigger efficiencies and the b-tagging scale factor. To obtain the systematic uncertainty from jet energy scale, we use the Higgs sample for a mass of 120 GeV. The jet energies in the WH MC samples are shifted by $\pm 1\sigma$ and the difference from the nominal acceptance is taken as the systematic uncertainty. The estimated value in one SECVTX tag w/ NNtag, double SECVTX tag and one SECVTX tag plus Jet Probability tag is 2.3, 2.5 and 2.8% using only 2 jet bin, respectively.

Lepton ID and trigger systematics are estimated in [7, 8, 9, 10]. These systematics uncertainties are calculated for each run range and combined using a luminosity weighted average. $\sim 2\%$ is assigned as Lepton ID systematic uncertainty. The uncertainty for the trigger efficiency is estimated to be less than one percent.

ISR and FSR systematic uncertainty are estimated by changing the parameters related to ISR and FSR from default values to half and double. Half of difference between the two samples is taken as the systematic uncertainly. The estimated values in one SECVTX tag w/ NNtag, ST+ST, ST+JP stage are 2.1%, 4.5% and 2.7% and 2.0%, 2.7% and 2.9% ,respectively (include MC statistics). and the combination of these uncertainties 2.9%, 5.2% and 4.0% is taken as ISR/FSR total systematic uncertainty.

PDFs uncertainties are evaluated using the standard re-weighting method recommended by Joint Physics [10]. The estimated value in one SECVTX tag w/ NN tag, ST+ST and ST+JP stage is 1.2%, 2.1% and 1.5%, respectively.

The b-tagging scale factor uncertainty comes from the High p_T b-tagging group. Propagating this uncertainty through our analysis, we estimate an acceptance uncertainty of 5.6%, 10.6% and 10.5% for one SECVTX tag w/ NN tag and 10.5% for double SECVTX tag and one SECVTX plus Jet Probablity. Total systematic uncertainties are listed in Table.10 for each b-tagging category.

Luminosity uncertainties are also included in calculating Higgs signal events. This uncertainty assign 6%.

Note: Previous versions of this analysis suggest that the acceptance systematics are much larger than the shape systematics. Therefore, at this time, we've focused on the acceptance systematics. In the near future, we will check this assumption by evaluating shape systematics.

6 Neural Network Discriminant

To further improve signal to background discrimination after event selection, we employ an artificial Neural Network (NN) trained on a variety of kinematic variables to distinguish WH from backgrounds. We use the RootJetnet interface to the Jetnet neural network program.

To optimize the NN, we use an iterative procedure to determine the configuration which best discriminates signal and background, and which uses a minimal number of input discriminants. The $1fb^{-1}$ ZH analysis [17] used the same optimization procedure. This is done by first determining the best one-variable NN from a list of 36 possible choices. The optimization algorithm keeps this variable as an input, the loops over all other the variables to determine the best two-variable NN. The best N-variable network is finally selected once the N+1-variable network shows less than a percent improvement. The criteria for comparing networks is the testing error defined by how often an NN with a given configuration correctly classifies several thousand signal and background events.

We optimized the NN structure on signal sample with M(H)= 120 GeV. We used the optimal structure of input variables to train sepearte neural networks for Higgs masses of 110, 115, 120, 130, 140, and 150. Re-training networks with the same structure and different signal masses keeps the neural net sensitivity constant as a function of higgs mass. We expect that this constant increase in sensitivity versus mass is also an optimal increase. Further studies could investigate whether other combinations of input variables becomes more powerful at different Higgs masses.

Our final Neural Network configuration has 3 input variables, 4 hidden nodes, and 1 output node. The 3 optimal inputs are,

- *Dijet Mass* : The invariant mass of the jet-jet system.
- P_T *imbalance* : $P_T(jet_1) + P_T(jet_2) + P_T(lep) - \not{E}_T$, the difference between the $\not{E}_T$ and the sum of the P_T of the other objects in the event
- $P_T(W + H)$: $P_T(\vec{lep} + \vec{\nu} + \vec{jet}_1 + \vec{jet}_2)$, The total P_T of the WH system.

Figures 12 to 14 shows the correlations between different pairs of NN inputs for WH signal and the background used for training the NN.

Figure 15 shows unit normalized shape comparison plots between the NN inputs. Figure 16 shows the shape comparison between the NN outputs.

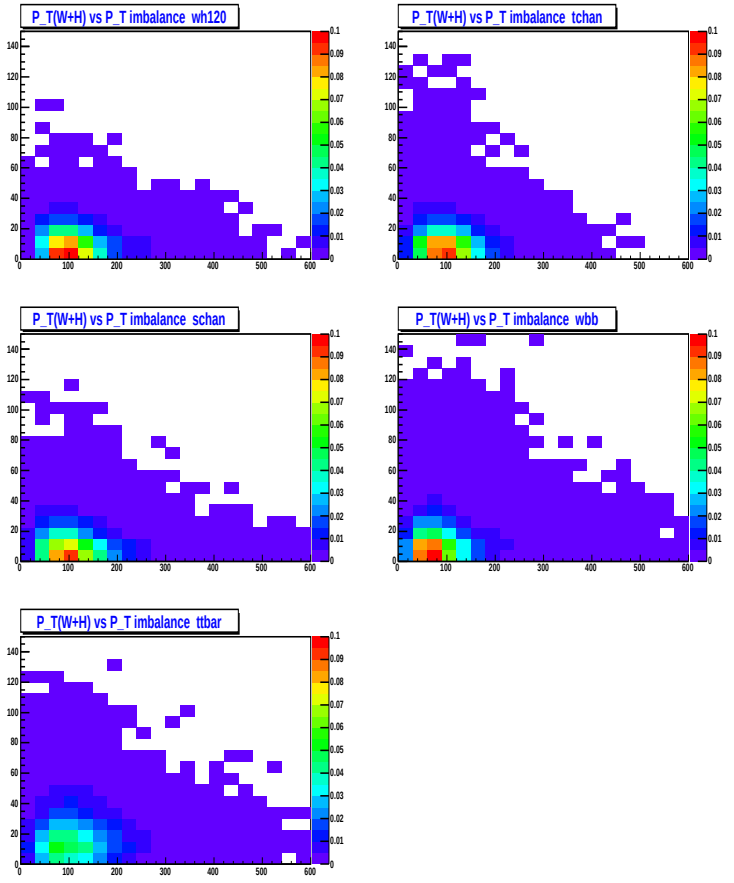

Figure 12: $P_T(W+H)$ vs P_T *imbalance* for WH (M=120) and major backgrounds. Each plot normalized to unit area. The scale on the z-axis is the same for all plots.

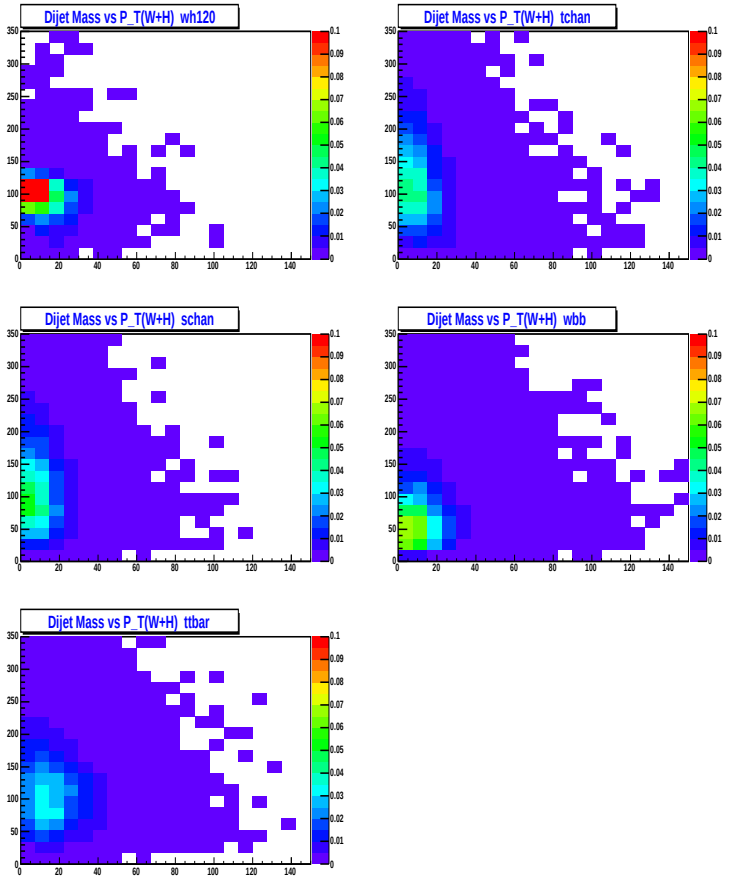

Figure 13: *Dijet Mass* vs $P_T(W+H)$ for WH (M=120) and major backgrounds. Each plot normalized to unit area. The scale on the z-axis is the same for all plots.

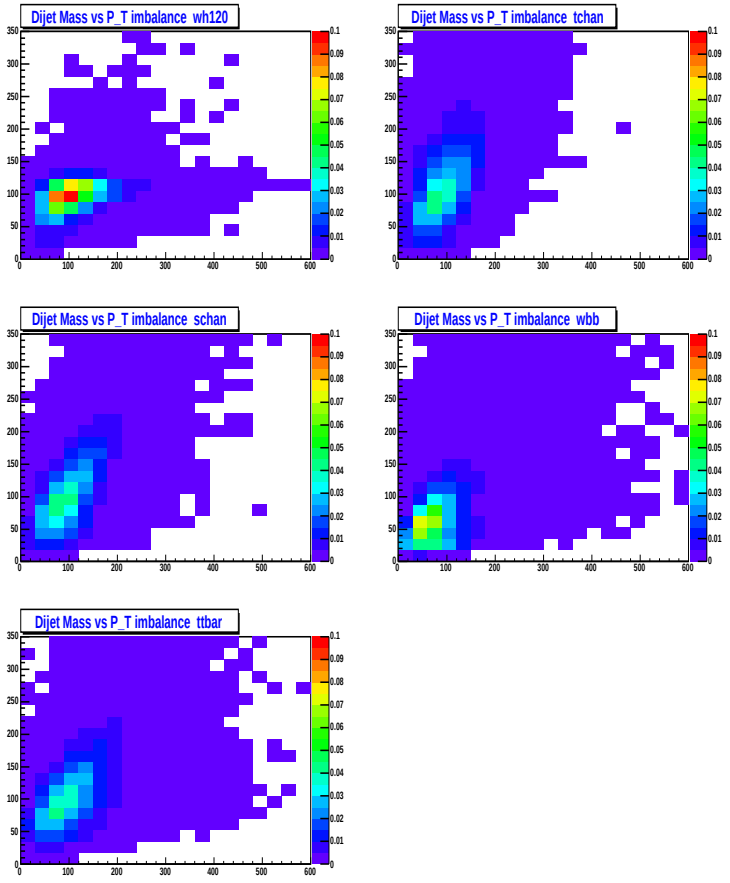

Figure 14: *Dijet Mass* vs P_T *imbalance* for WH (M=120) and major backgrounds. Each plot normalized to unit area. The scale on the z-axis is the same for all plots.

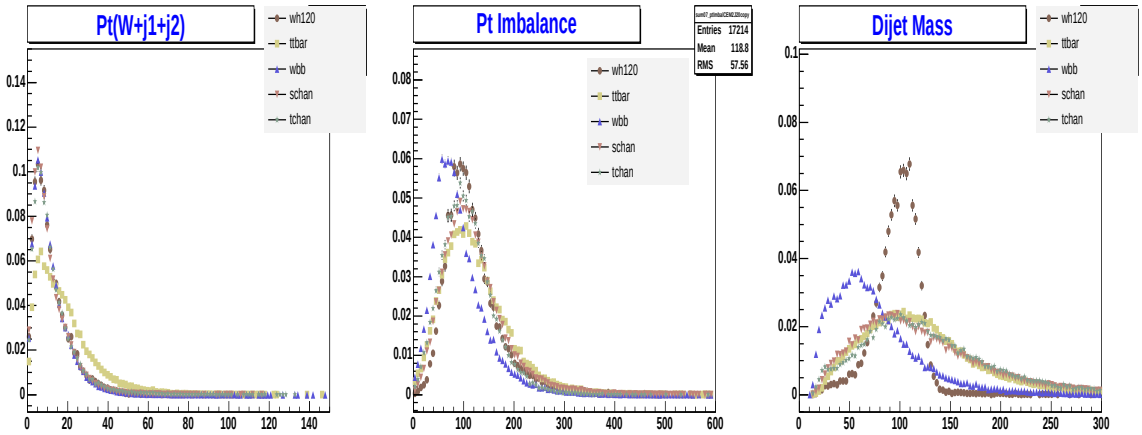

Figure 15: Comparison of NN input variable kinematics for signal (M(H)=120) and major backgrounds. Each histogram is normalized to unit area.

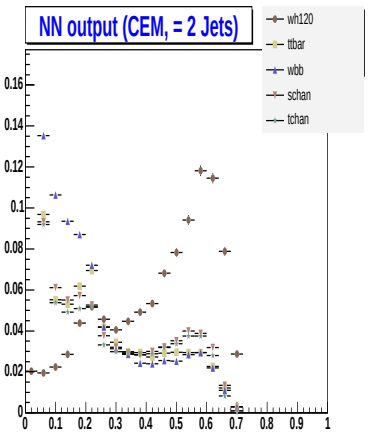

Figure 16: Comparison of NN output for signal (M(H)=120) and major backgrounds. Each histogram normalized to unit area.

7 Kinematic shape

We check the kinematics for each tagging category to make sure that the background compositions are well understood between data and Monte Carlo. The non-W shape is derived directly from data using C region ($\not\!\!E_T$ >20 GeV and lepton isolation > 0.1). The W+jets shape is determined from Monte Carlo using ALPGEN_v2 and is normalized to the data after subtracting other backgrounds in pretag. The mistag shape is obtained from the data events before tagging, but weighted by the mistag matrix. The rest of the backgrounds, such as $t\bar{t}$, single top and diboson, are derived from Monte Carlo simulation with a top mass of 175 GeV/c^2. We add signal shape for each tagging category after scaling to able to see signal shape.

7.1 pretag

Figures 17-22 show the fundamental observed and expected shapes of lepton, Missing energy and two jets and correlation between these variables in the pretag sample in the W+2jet bin. As we mentioned, the background estimation is normalized to the number of events observed in the data. These plots show good agreement between the data and the background prediction.

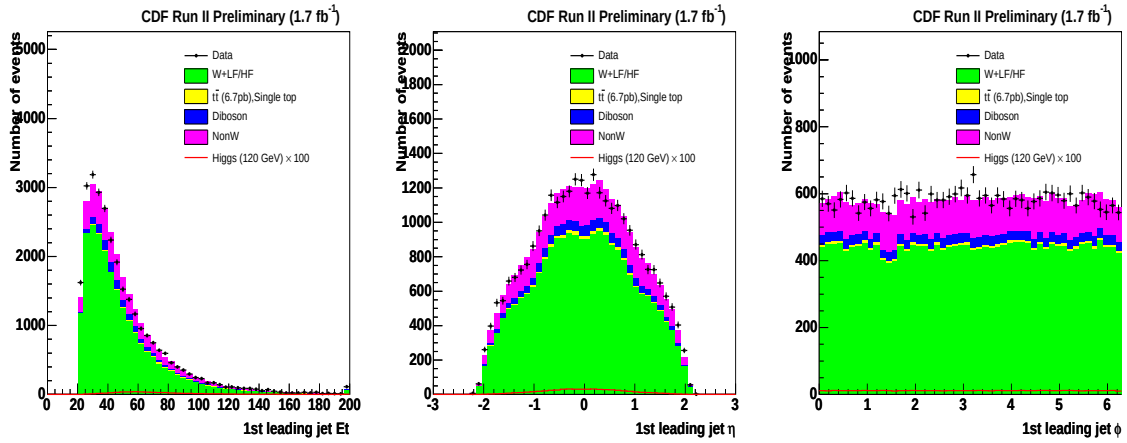

Figure 17: The first leading jet E_T, η and ϕ kinematic distributions in the pretag events. The W+jets background is normalized to the data after subtracting other backgrounds.

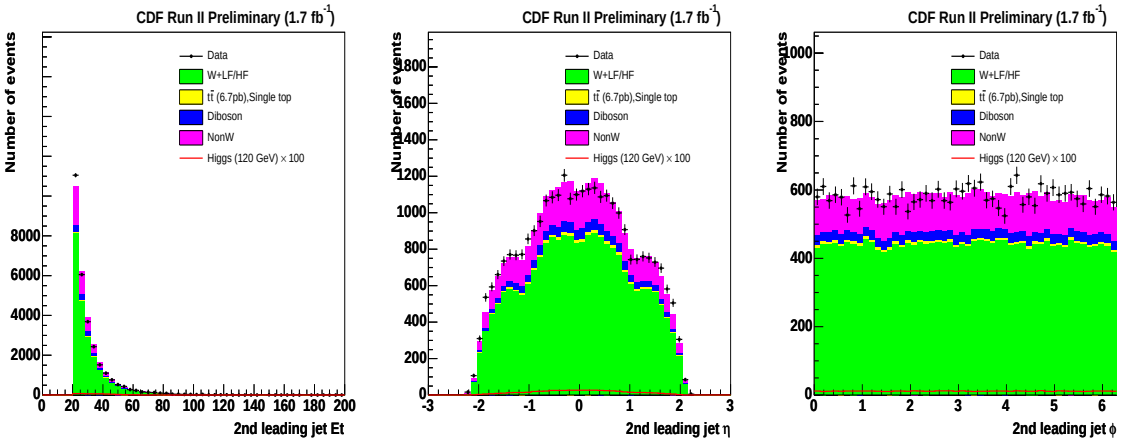

Figure 18: The second leading jet E_T, η and ϕ kinematic distributions in the pretag events. The W+jets background is normalized to the data after subtracting other backgrounds.

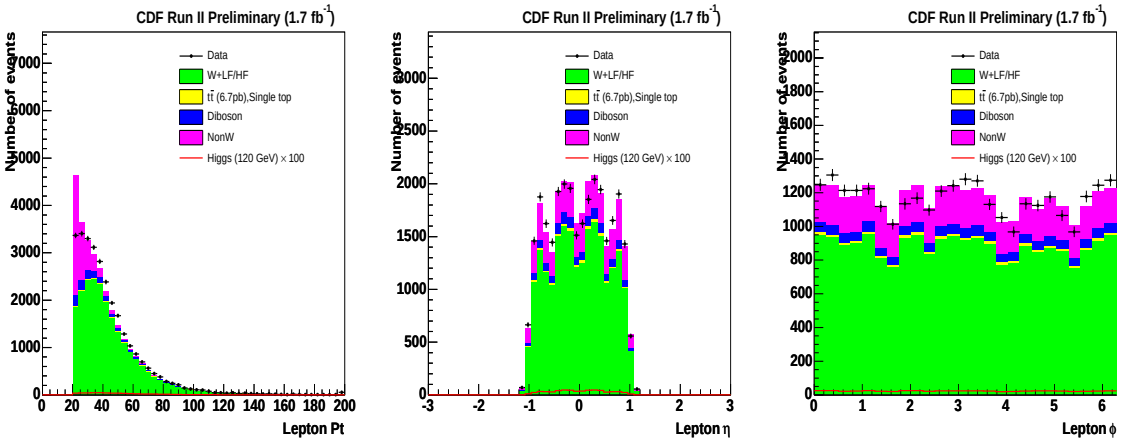

Figure 19: The lepton P_T, η and ϕ kinematic distributions in the pretag events. The W+jets background is normalized to the data after subtracting other backgrounds.

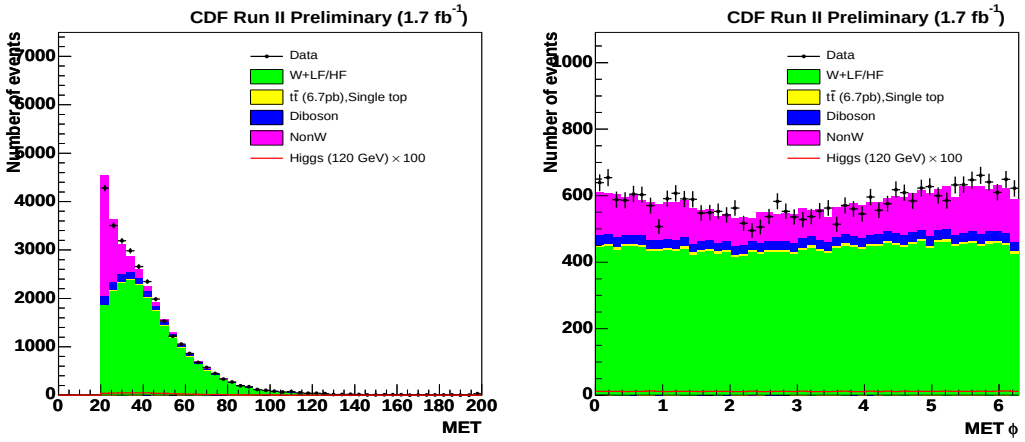

Figure 20: The $\not\!\!E_T$ and ϕ kinematic distributions in the pretag events. The W+jets background is normalized to the data after subtracting other backgrounds.

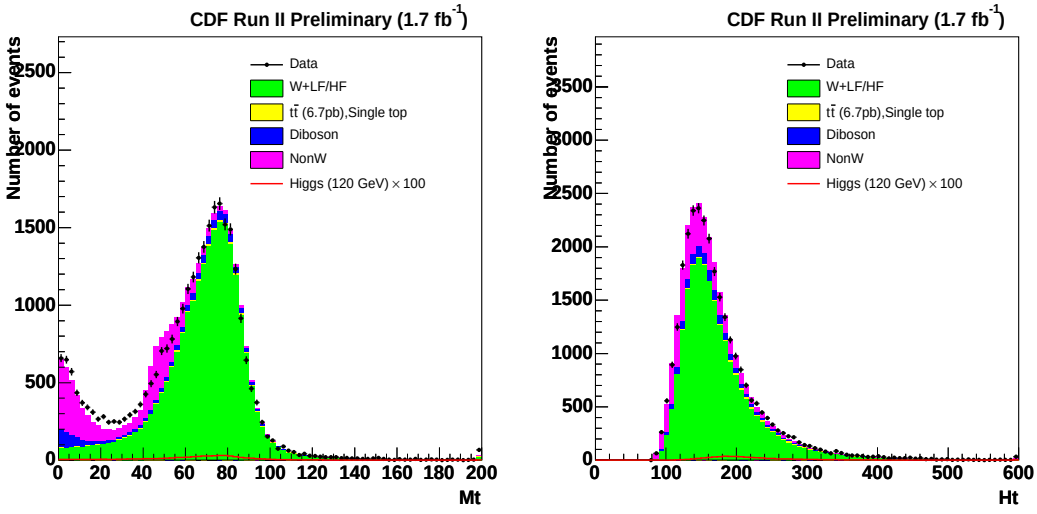

Figure 21: The reconstructed W transverse mass and Ht distributions in the pretag events. The W+jets background is normalized to the data after subtracting other backgrounds.

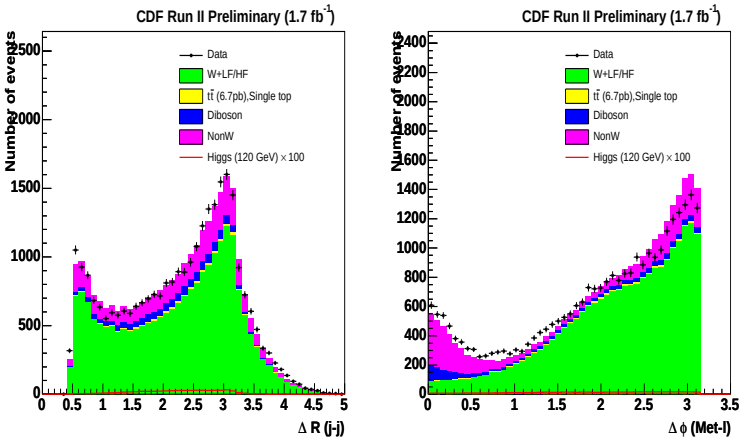

Figure 22: The observed and expected ΔR between dijet and $\Delta\phi$ between $\not\!\!E_T$ and lepton in the pretag events. The W+jets background is normalized to the data after subtracting other backgrounds.

7.2 One SECVTX tag w/ NNtag

Figures 23-28 show similar plots for events with at least one tight SECVTX tag in W+2jet bin where the backgrounds are normalized according to their Method 2 expectations and the Method 2 uncertainties are shown.

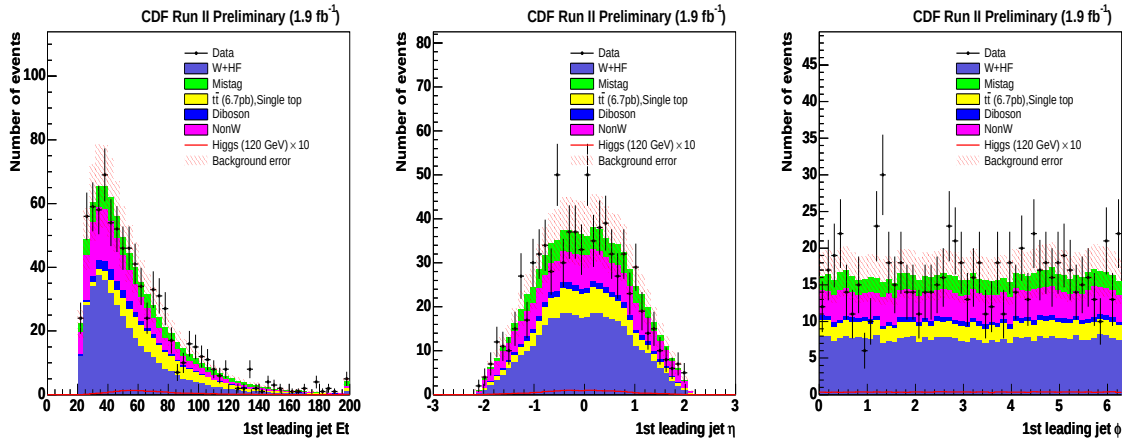

Figure 23: First leading jet E_T, η and ϕ kinematic plots in one SECVTX w/ NN tagged events. Background uncertainty is shown in red hash.

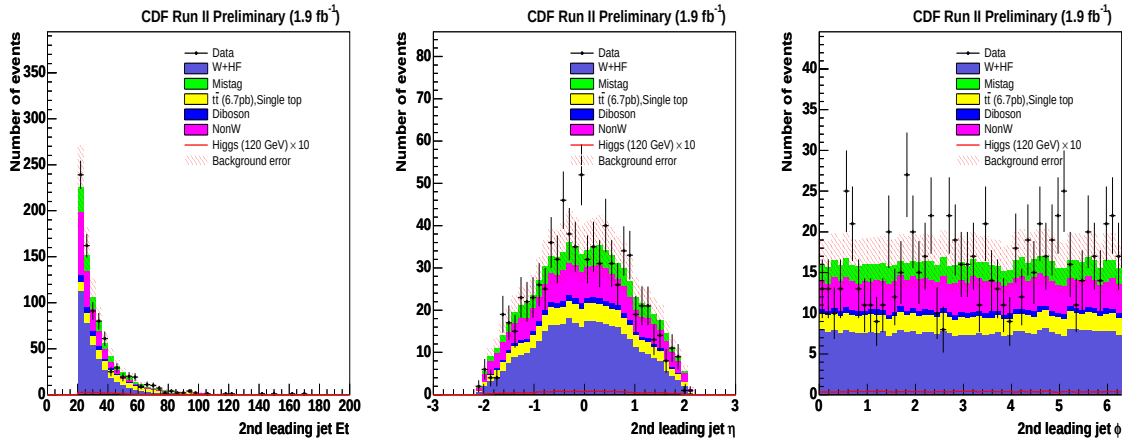

Figure 24: Second leading jet E_T, η and ϕ kinematic plots in one SECVTX w/ NN tagged events. Background uncertainty is shown in red hash.

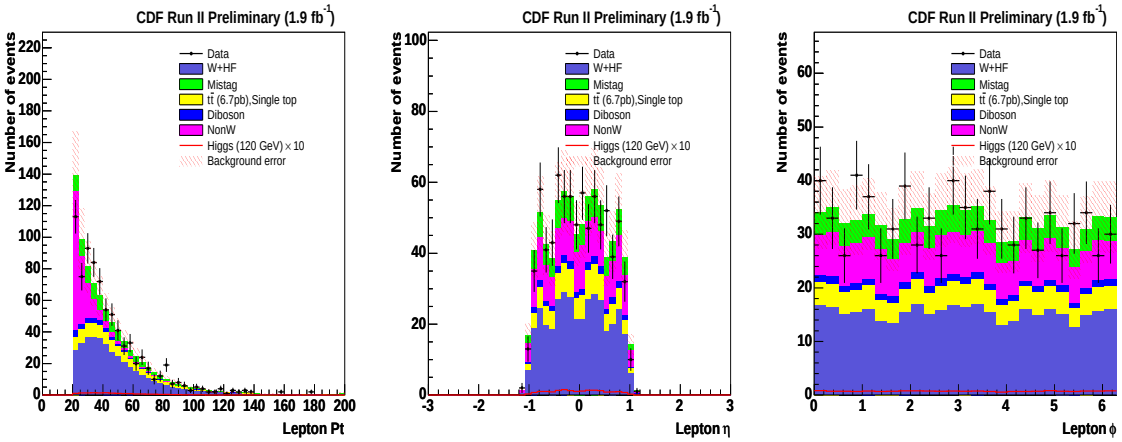

Figure 25: Lepton P_T, η and ϕ kinematic plots in one SECVTX w/ NN tagged events. Background uncertainty is shown in red hash.

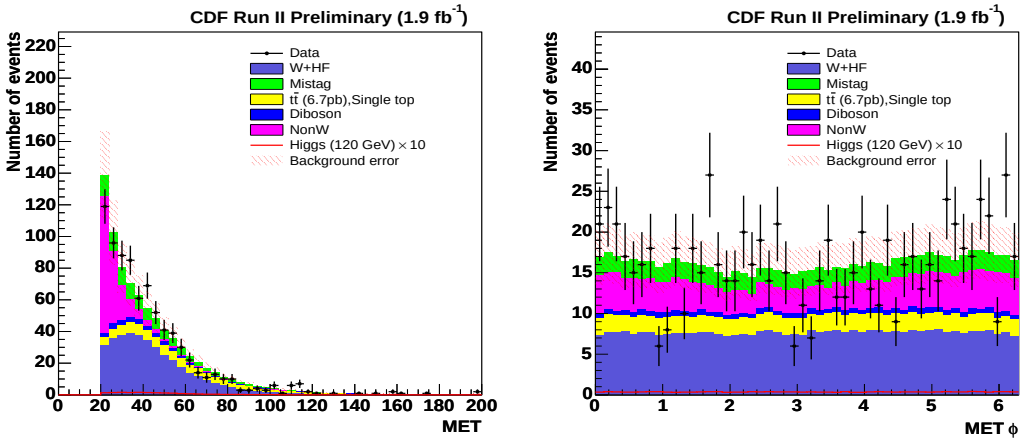

Figure 26: $\not\!\!E_T$ and ϕ kinematic plots in one SECVTX w/ NN tagged events. Background uncertainty is shown in red hash.

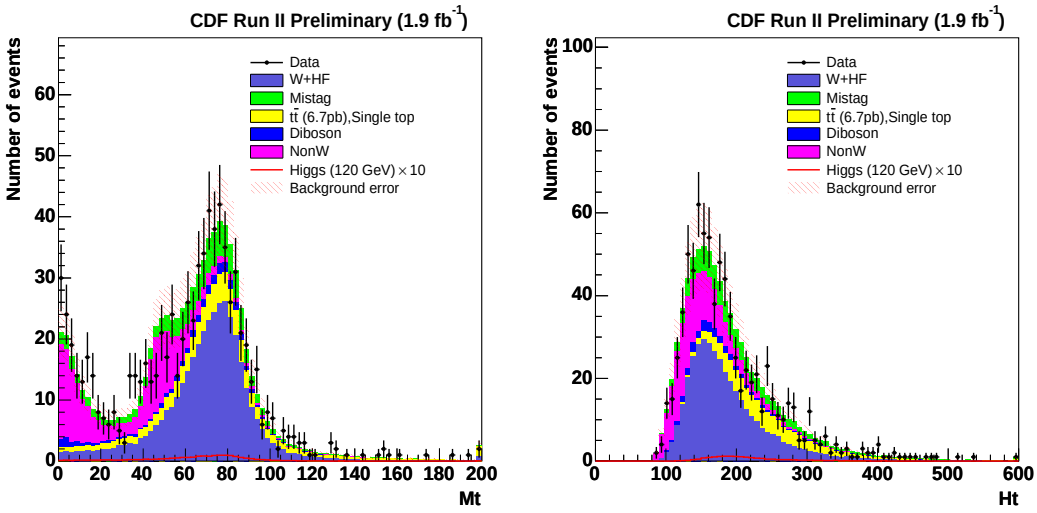

Figure 27: Transverse mass of W and Ht plots in one SECVTX w/ NN tagged events. Background uncertainty is shown in red hash.

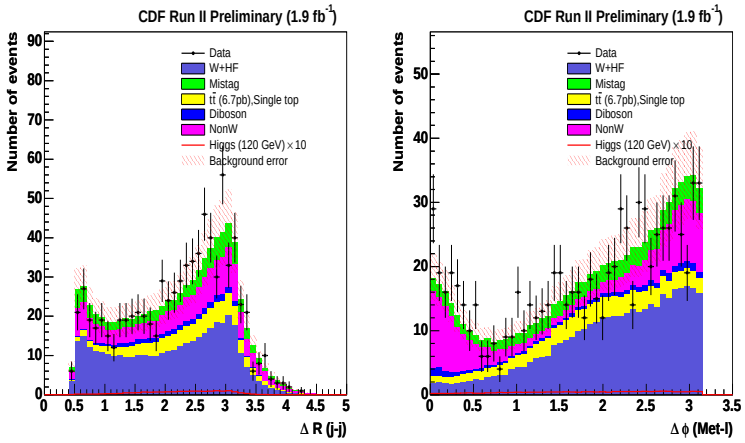

Figure 28: From left, ΔR between dijet and $\Delta\phi$ between $\not\!\!E_T$ and lepton in one SECVTX w/ NN tagged events. Background uncertainty is shown in red hash.

7.3 Double SecVtx tag

Figures 29-34 show the observed and expected kinematic distributions in the double SecVtx tagged events in W+2jet bin. Again, our data and the background model agree within the statistical uncertainty on the data.

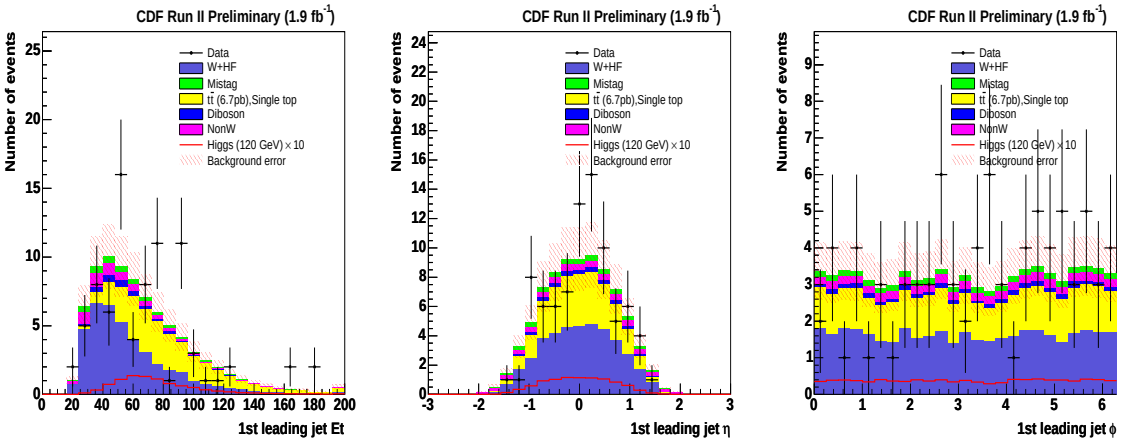

Figure 29: First leading jet E_T, η and ϕ kinematic plots in double SecVtx tagged events. Background uncertainty is shown in red hash

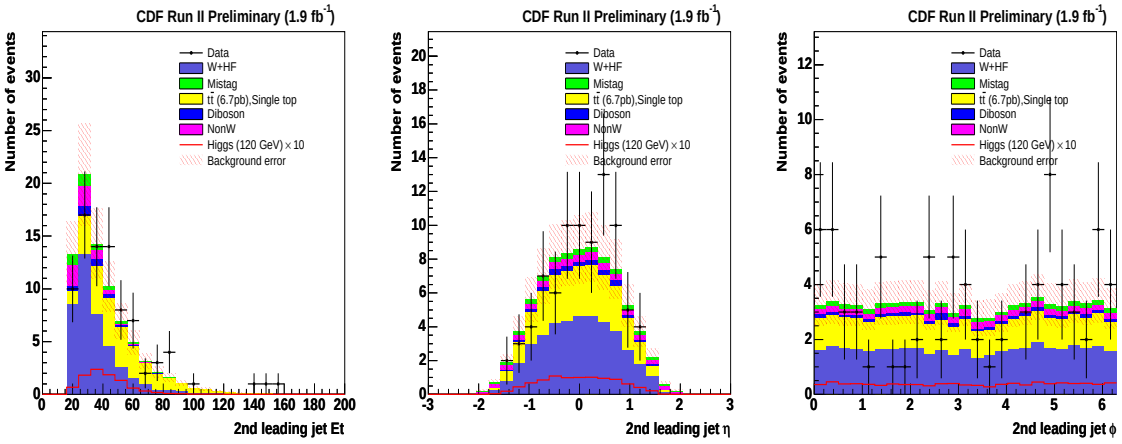

Figure 30: Second leading jet E_T, η and ϕ kinematic plots in double SecVtx tagged events. Background uncertainty is shown in red hash.

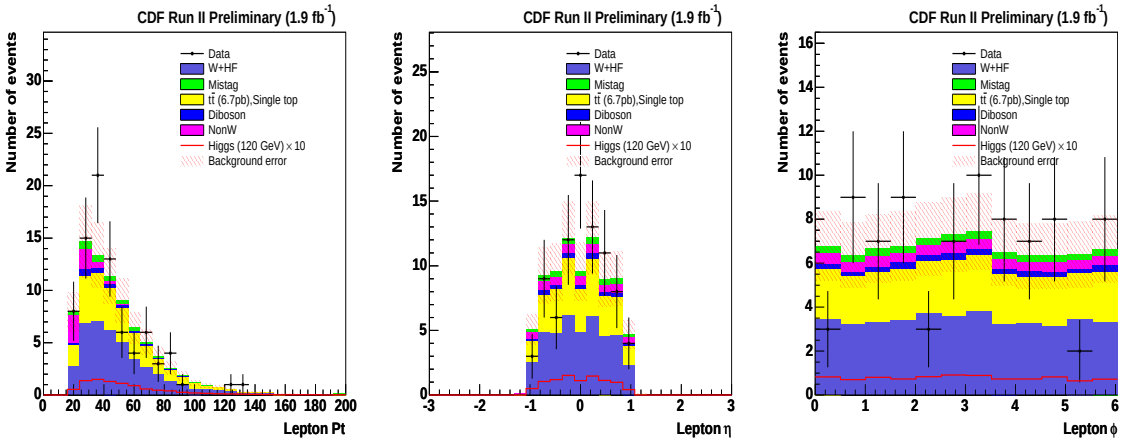

Figure 31: Lepton P_T, η and ϕ kinematic plots in double SecVtx tagged events. Background uncertainty is shown in red hash.

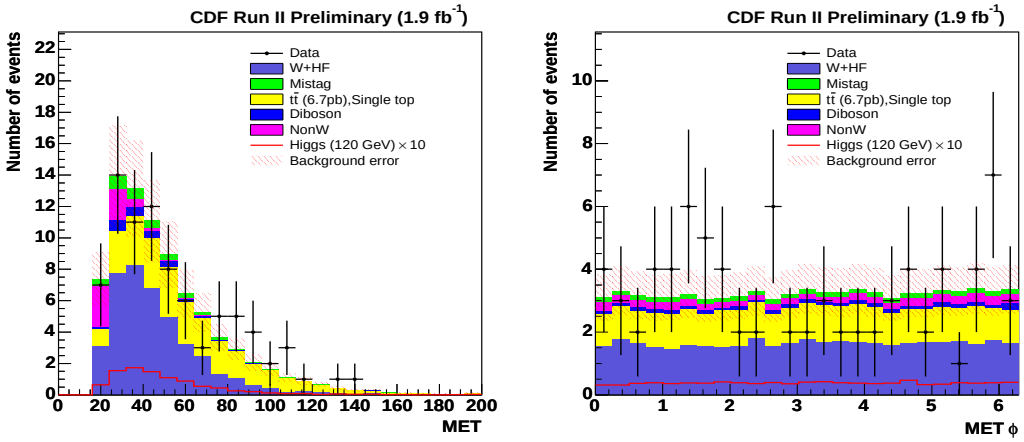

Figure 32: $\not\!\!E_T$ and ϕ kinematic plots in double SecVtx tagged events. Background uncertainty is shown in red hash.

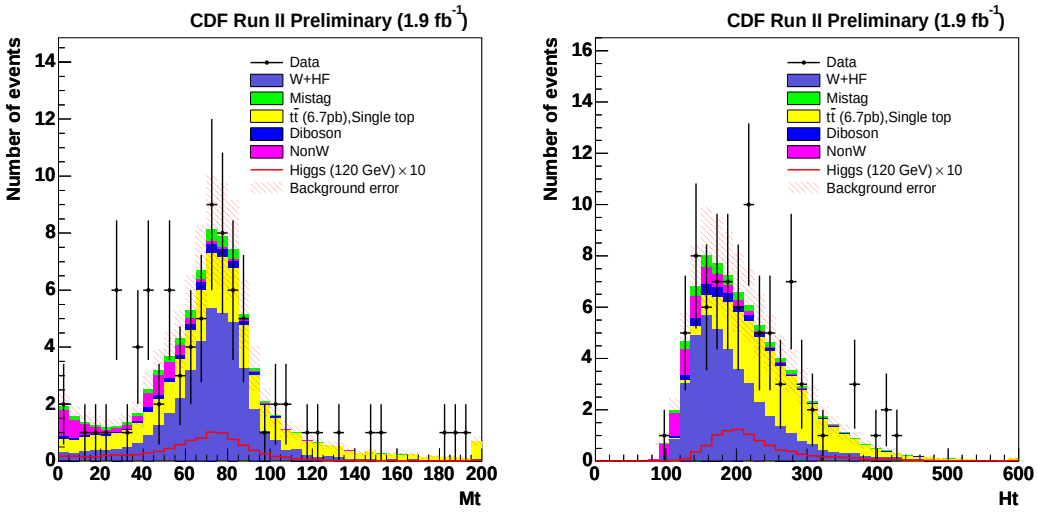

Figure 33: Transverse mass of W and Ht plots in double SecVtx tagged events. Background uncertainty is shown in red hash.

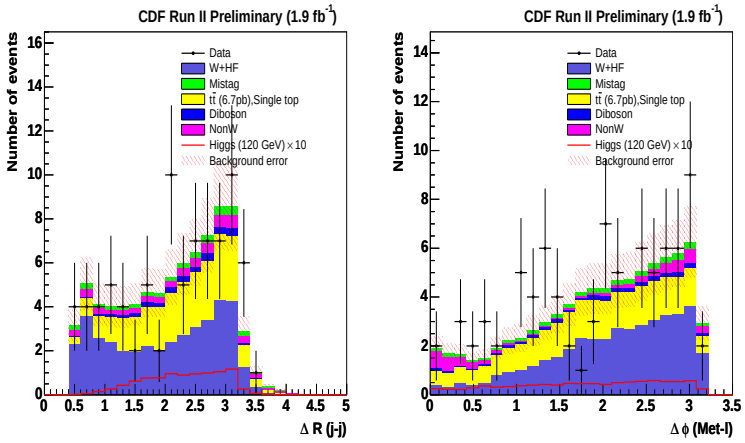

Figure 34: From left,ΔR between dijet and $\Delta\phi$ between $\not\!\!E_T$ and lepton in double SecVtx tagged events. Background uncertainty is shown in red hash.

7.4 One SecVtx tag and One Jet probability tag

Figures 35-40 show the observed and expected kinematic shapes in the double tagged events with one SECVTX tag + one jet probability tag in W+2jet bin. Again, the agreement between the two is excellent although the statics are not great.

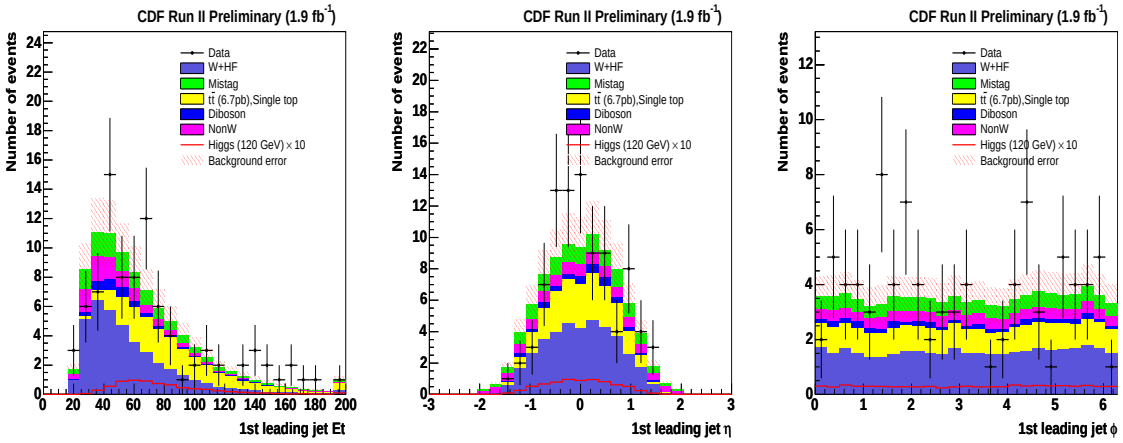

Figure 35: First leading jet E_T, η and ϕ kinematic plots in one SecVtx tag and one Jet probability tag events. Background uncertainty is shown in red hash.

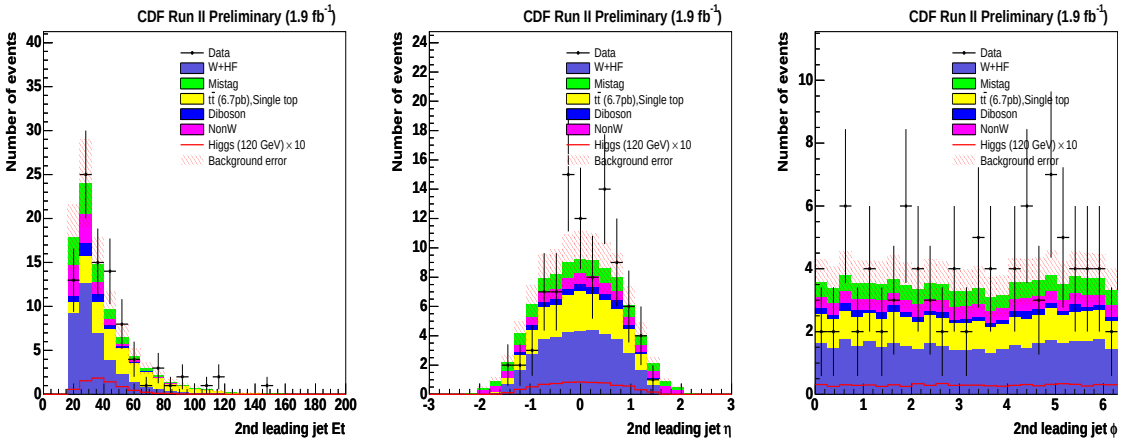

Figure 36: Second leading jet E_T, η and ϕ kinematic plots in one SecVtx tag and one Jet probability tag events. Background uncertainty is shown in red hash.

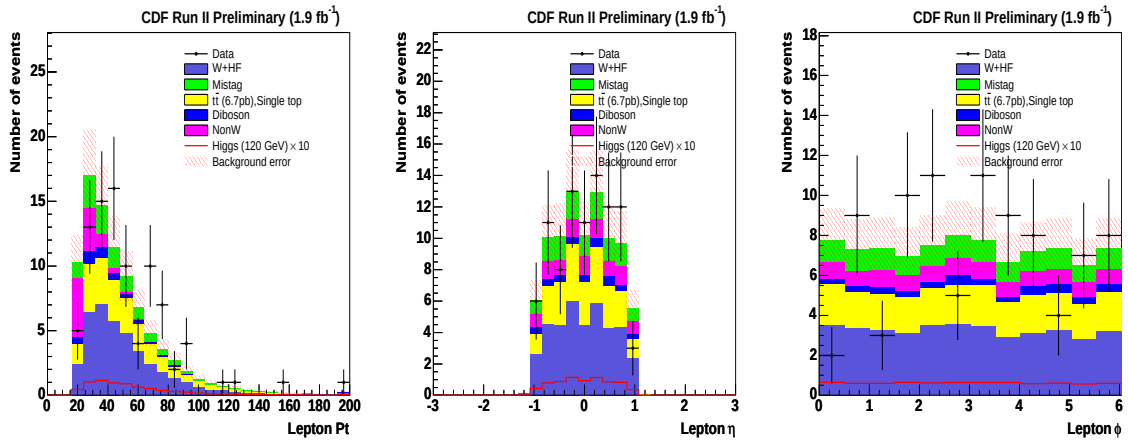

Figure 37: Lepton P_T, η and ϕ kinematic plots in one SecVtx tag and one Jet probability tag events. Background uncertainty is shown in red hash.

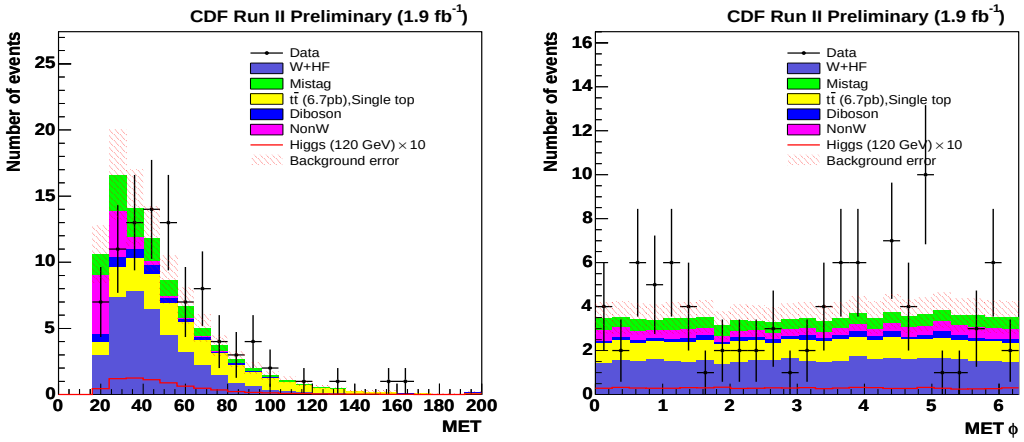

Figure 38: $\not\!\!E_T$ and ϕ kinematic plots in one SecVtx tag and one Jet probability tag events. Background uncertainty is shown in red hash.

8 NN kinematic shape

Figures 41-48 shows the NN input variables and output shape for each tagging category. First we check whether the all NN input variables are modeled reasonably and consistent with observed data for each tagging categories. As described in Section 6, the Higgs signal ideally produces a high NN output value while the backgrounds produce low values. Finally NN output distribution for each tagging category is shown to search for the Standard Model Higgs boson.

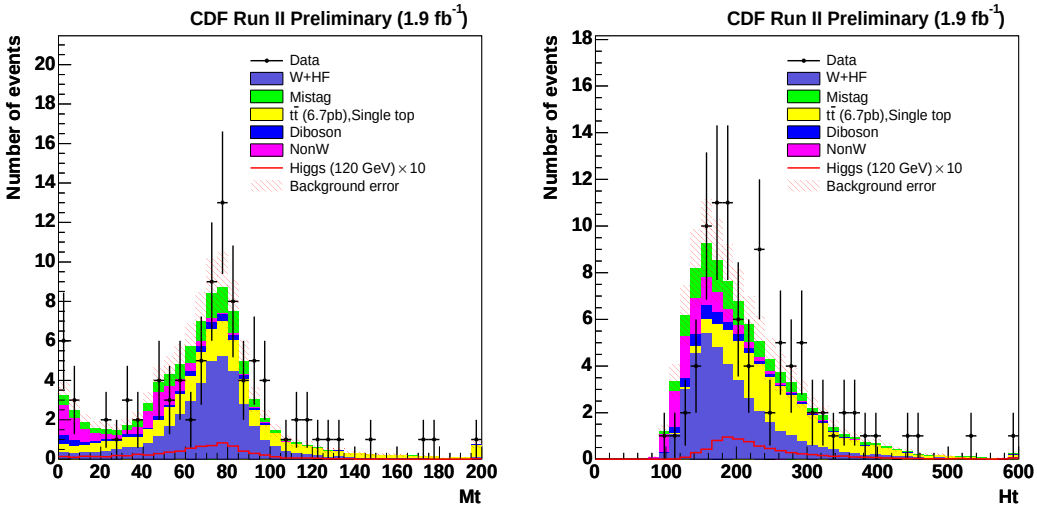

Figure 39: Transverse mass of W and Ht plots in one SecVtx tag and one Jet probability tag events. Background uncertainty is shown in red hash.

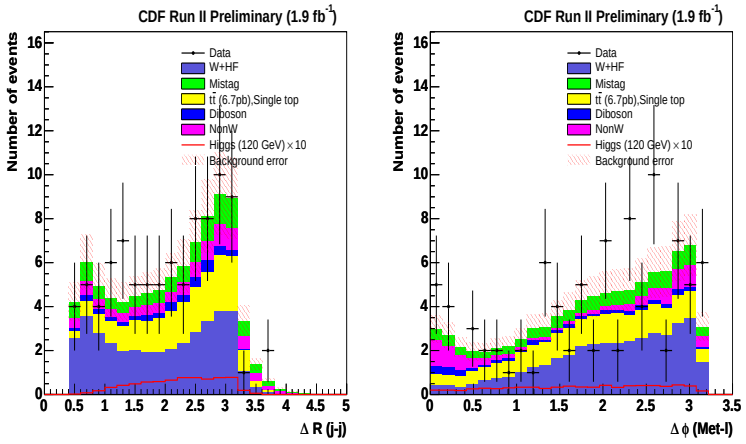

Figure 40: From left, ΔR between dijet and $\Delta\phi$ between $\not\!\!E_T$ and lepton in one SecVtx tag and one Jet probability tag events. Background uncertainty is shown in red hash.

8.1 pretag

Figures 41 show the NN input variables, Met Imbalance, Pt of W+2jet system and dijet mass distribution. The total background number is normalized to data using W+jets events in pretag events. Figure 42 shows the NN output distributions calculated from three NN input variables. The expected background shape is consistent with observed background shape.

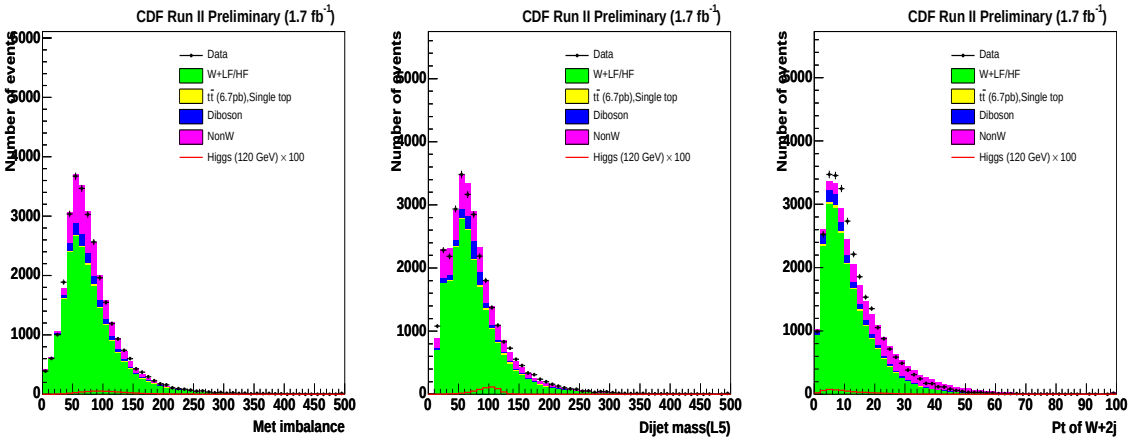

Figure 41: The observed and expected NN input variables, Met Imbalance and Dijet mass reconstructed by Jet energy correction L5 and Pt of W+2jet system in the pretag events. The W+jets background is normalized to the data after subtracting other backgrounds.

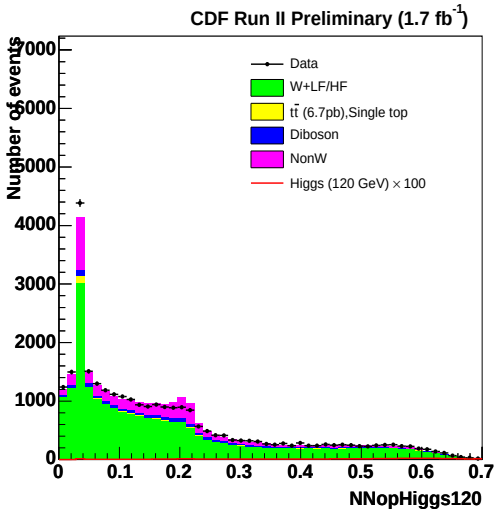

Figure 42: NN output shape calculated from three input variables for pretag events. Higgs signal should produce high NN output values.

8.2 one tag w/ NNtag

Figures 43 show the NN input variables, Met Imbalance, Pt of W+2jet system and dijet mass distribution for one SECVTX tag w/ NN tagged events. Figure 44 shows the NN output distributions calculated from three NN input variables. The expected background shape is consistent with observed background shape.

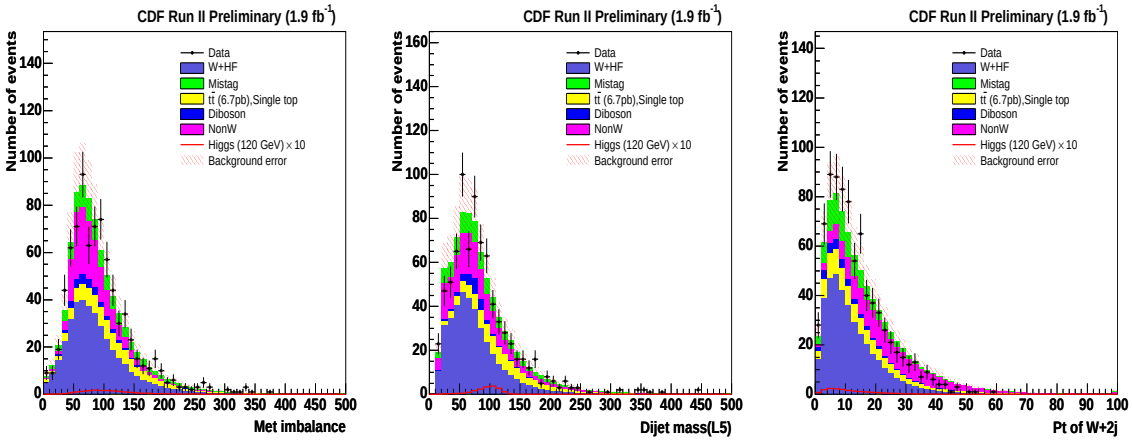

Figure 43: The observed and expected NN input variables, Met Imbalance and Dijet mass reconstructed by Jet energy correction L5 and Pt of W+2jet system in one SECVTX w/ NN tag.

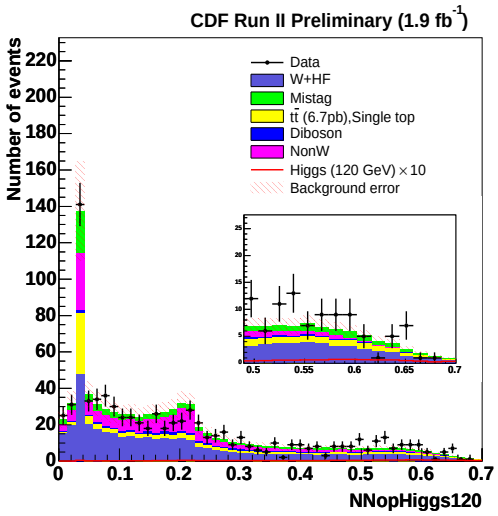

Figure 44: NN output shape calculated from three input variables for double tight SecVtx category. NN output shape is calculated for each signal mass points. Higgs signal should produce high NN output values.

8.3 Double SECVTX tag

Figures 45 show the NN input variables, Met Imbalance, Pt of W+2jet system and dijet mass distribution for double SECVTX tagged events. Figure 46 shows the NN output distributions calculated from three NN input variables. The expected background shape is consistent with observed background shape.

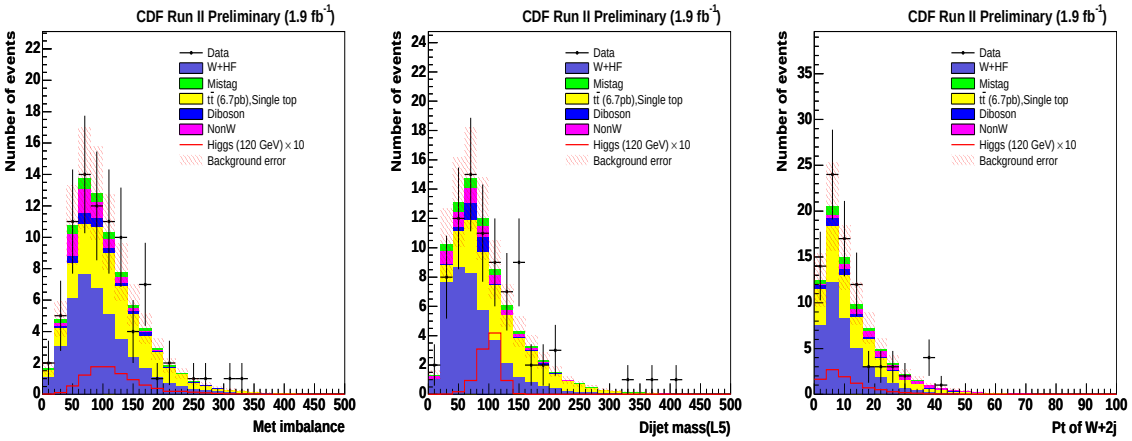

Figure 45: The observed and expected NN input variables, Met Imbalance and Dijet mass reconstructed by Jet energy correction L5 and Pt of W+2jet system in the double tight SecVtx tag.

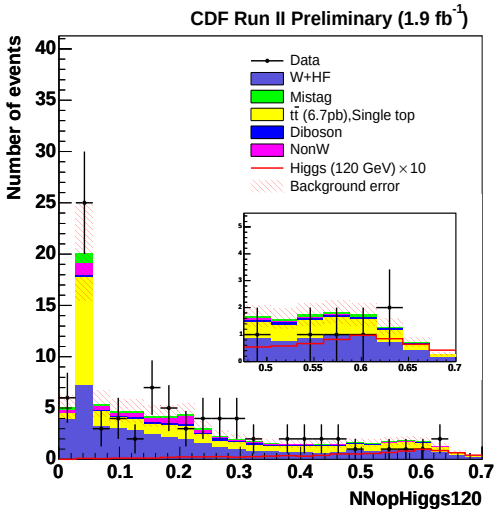

Figure 46: NN output shape calculated from three input variables for double tight SECVTX category. NN output shape is calculated for each signal mass points. Higgs signal should produce high NN output values.

8.4 One SECVTX plus Jet Probability tag

Figures 47 show the NN input variables, Met Imbalance, Pt of W+2jet system and dijet mass distribution for one SECVTX plus Jet Probability tagged events. Figure 48 shows the NN output distributions calculated from three NN input variables. The expected background shape is consistent with observed background shape.

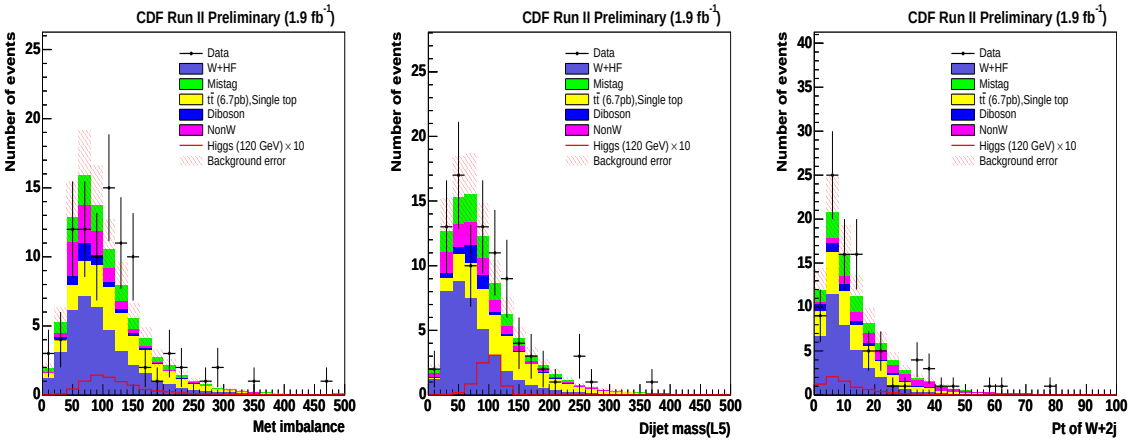

Figure 47: The observed and expected NN input variables, Met Imbalance and Dijet mass reconstructed by Jet energy correction L5 and Pt of W+2jet system in one SECVTX plus Jet Probability tag.

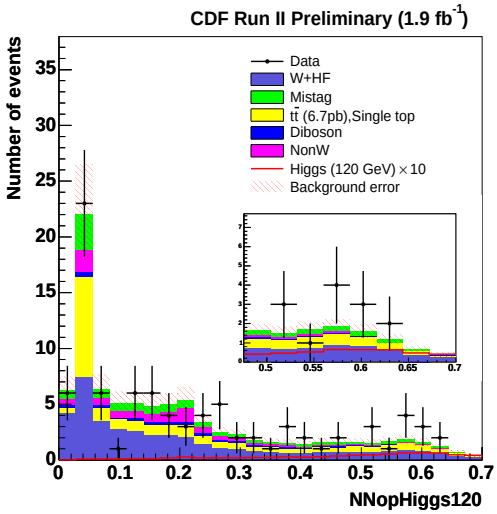

Figure 48: NN output shape calculated from three input variables for one SECVTX tag plus Jet Probability. NN output shape is calculated for each signal mass points. Higgs signal should produce high NN output values.

9 Sensitivity and 95% C.L. upper limit: Dijet Invariant Mass

Since there is no significant excess of events in the data compared to the background expectation, we fit the NN output distribution and extract the expected 95% C.L. upper limit for various b-tagging strategies using pseudo-experiments based on the background expectations.

9.1 Binned Likelihood Technique

We set an upper limit on the production cross section times branching ratio of $p\bar{p} \to WH$ as a function of m_h by using the number of events in the $W^{\pm} + 2$ jets sample. Since there are no peaks observed from NN ouput distribution, we assume that the $W^{\pm} + 2$ jets and dijet mass distributions in the data consist of QCD (mistags, $W^{\pm} + b\bar{b}$, $W^{\pm} + c\bar{c}$, $W^{\pm} + c$ Z+jets and diboson), TOP ($t\bar{t}$ and single top) and WH higgs signal events. A 1-dimensional binned maximum likelihood technique is used to obtain the limit on the cross section of signal process as in the previous analysis. The expected number of events (μ_i) in each mass bin is

$$\mu_i = f_i^{QCD} \cdot N^{QCD} + f_i^{TOP} \cdot N^{TOP} + f_i^{WH \to l\nu b\bar{b}} \cdot (\varepsilon \cdot \mathcal{L} \cdot \sigma_{WH \to l\nu b\bar{b}}),$$

where f_i^{QCD}, f_i^{TOP} and $f_i^{WH \to l\nu b\bar{b}}$ are the expected fraction of events in a given mass bin predicted by Monte Carlo. N^{QCD}, N^{TOP}, ε, $\mathcal{L}$ and $\sigma_{WH \to l\nu b\bar{b}}$ are the expected number of QCD and TOP events, the detection efficiency, the luminosity and the unknown $WH \to l\nu b\bar{b}$ cross section respectively. In pseudo-experiment, to make the pseudo-data, we fluctuate the number of expected QCD and Top with Gaussian with the estimated total uncertainty independently, and also signal events with total systematic uncertainty. Then the corresponding likelihood is

$$L(\sigma \times BR) = \iiint \prod_{i=bin} \frac{\mu_i^{N_i} \cdot e^{-\mu_i}}{N_i!} G(N_{QCD}, \sigma_{N_{QCD}}) G(N_{TOP}, \sigma_{N_{TOP}}) G(N_{WH}, \sigma_{N_{WH}}) dN_{QCD} dN_{TOP} dN_{WH}, \quad (9)$$

We define the expected limit by taking the mean value of the iterated pseudo-experiment. We try to calculate the expected limit with each b-tag condition (double SECVTX tag, one SECVTX tag + Jet probability tag and one SECVTX tag w/ NN tag and double SECVTX tag & one SECVTX tag & one Jet probability tag combined and limit combined all tagging categories). The limit of "combined all tagging categories" are obtained by combining the three likelihood of L($\sigma|$ ST+ST), L($\sigma|$ST+JP) and L($\sigma|$ one tag w/ NNtag) as

$$L(\sigma) = L(\sigma|ST + ST) \times L(\sigma|ST + JP) \times L(\sigma|onetagw/NNtag)$$

where the correlation between b-tag categories is taken into account properly. The systematic uncertainty up to the pretag acceptance, luminosity uncertainty and uncertainty of SECVTX b-tag scale factor and Jet probability scale factor are considered to be 100% correlated between the three selection criteria.

Mass/b-tagging category	ST + ST	ST + JP	One SECVTX w/ NNtag
110 GeV	1.89 (11.7)	2.34 (14.5)	3.22 (19.9)
115 GeV	1.80 (13.7)	2.18 (16.6)	2.93 (22.3)
120 GeV	1.56 (15.3)	2.18 (21.3)	2.76 (27.1)
130 GeV	1.44 (23.1)	1.88 (30.2)	2.42 (38.8)
140 GeV	1.36 (44.4)	1.73 (56.7)	2.18 (71.2)
150 GeV	1.32 (112.6)	1.55 (132.0)	1.98 (168.9)

Table 11: This table shows upper limit using NN shape fitting for each mass point and each tagging category. The values in parentheses mean upper limit normalized to SM expectation

Mass/b-tagging category	ST +ST & ST + JP	1tag & 2tag
110 GeV	1.41 (8.7)	1.32 (8.2)
115 GeV	1.35 (10.3)	1.19 (9.0)
120 GeV	1.28 (12.5)	1.12 (11.0)
130 GeV	1.08 (17.3)	0.96 (15.4)
140 GeV	1.00 (32.8)	0.90 (29.3)
150 GeV	0.96 (82.2)	0.85 (72.8)

Table 12: This table shows combined upper limit using NN shape fitting for each mass point. The values in parentheses mean upper limit normalized to SM expectation

9.2 Expected Limit Result

We check the expected upper limit and decide the best limit a priori. Fig.49 shows upper limit on the production cross section times branching ratio. Fig. 50 shows upper limit normalized to SM cross section times branching ratio. Double SECVTX events has the best sensitivity in each one tagging category. Finally the best upper limit is obtained from the combined 1tag and 2 tag. Table 12 shows the expected limit obtained from selected tagging category for each Higgs mass. Table **??** shows the expected limit obtained from combination of selected tagging category for each Higgs mass. According to table, the gain by including 1tag w/ NN tag is 10% level.

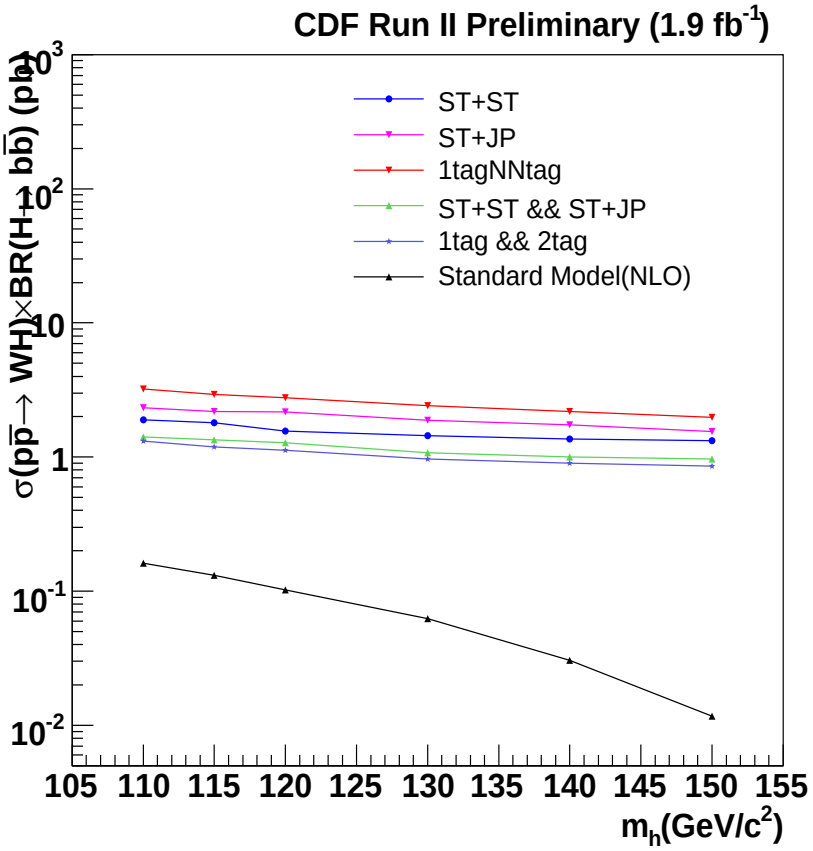

Figure 49: The 95% C.L. upper limit using the dijet invariant mass only estimated from pseudo experiments. Each color means each b-tagging strategy.

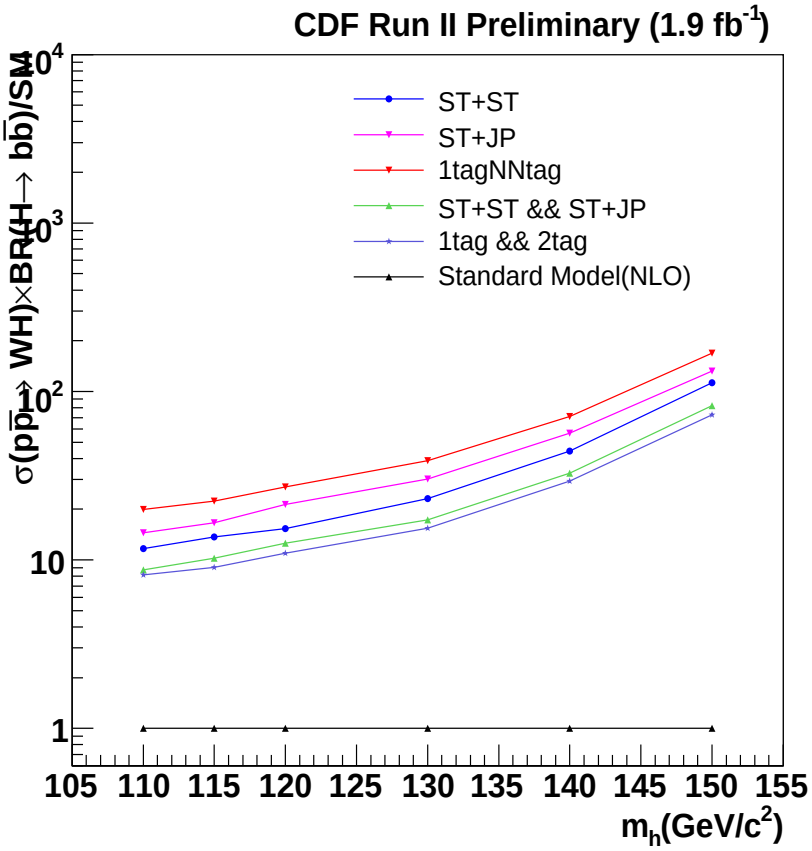

Figure 50: The ratio of 95% C.L. upper limit using the dijet invariant mass only to SM expectation. These values are estimated from pseudo experiments for each b-tagging strategy.

Figures 51-55 show distribution of 95% C.L. upper limit results from one thousand pseudo-experiments. The mean of these distribution is quoted as the central value for the expected limit and the RMS provides the 1 σ uncertainty band.

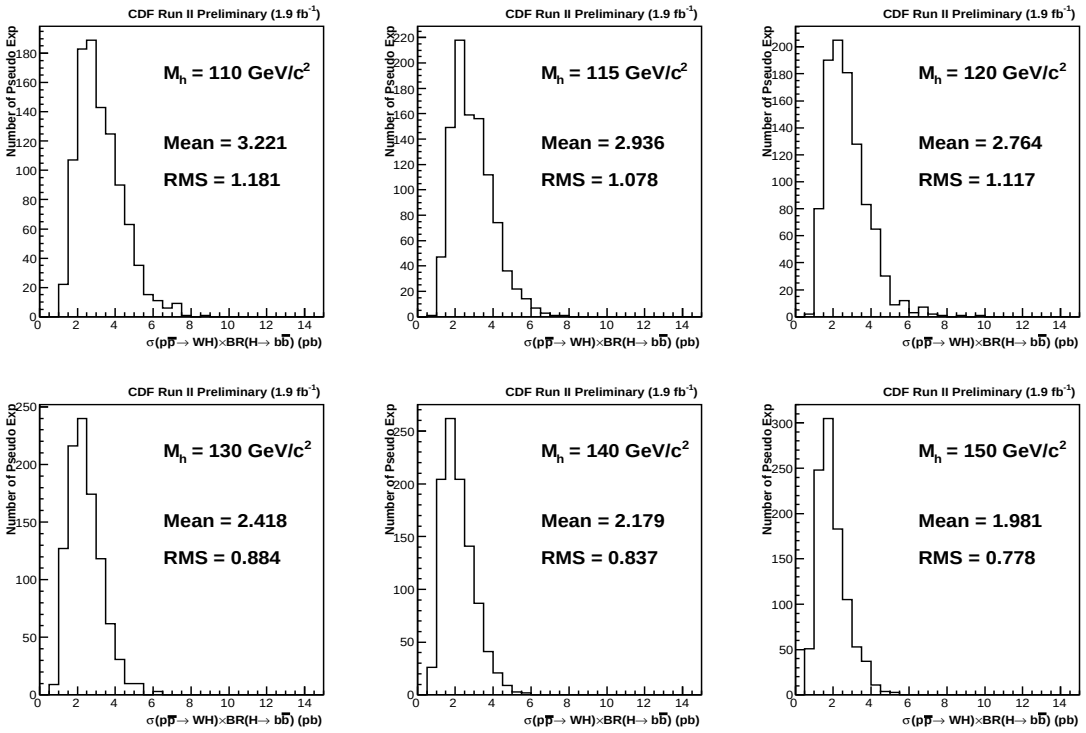

Figure 51: The results using NN output for one SECVTX tag w/ NNtag with one thousand pseudo experiments for each Higgs mass. The results show 95% C.L. upper limit for each pseudo experiment.

9.3 Observed limit

9.4 Neural Network Observed Limits

Figure 56 shows observed 95% C.L upper limit combined 1tag and 2tag for WH production cross section. Our observed limit is reasonable compared to pseudo experiment results. Figure 57 shows observed 95% C.L. upper limit for each tag cateogry. The observed limit for each tag category are good agreement to expected limit. In Table 14, the absolute and normalized by SM value of Observed limit values are shown.

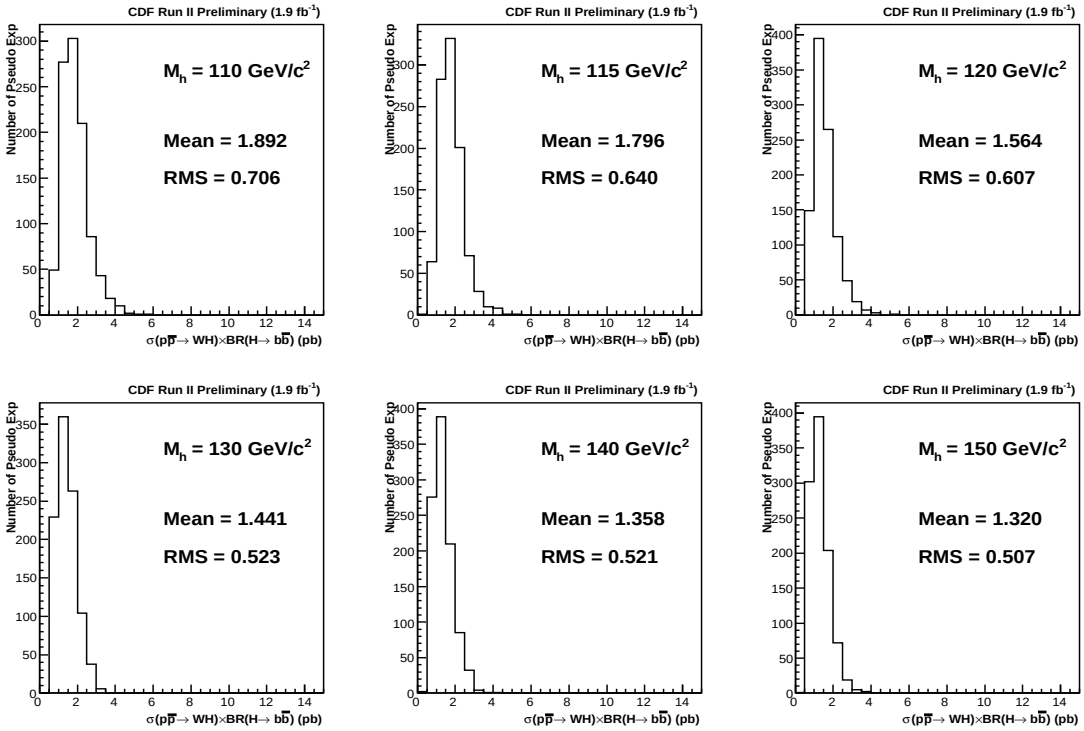

Figure 52: The results using NN output for double SECVTX tag with one thousand pseudo experiments for each Higgs mass. The results show 95% C.L. upper limit for each pseudo experiment.

Mass/b-tagging category	ST + ST	ST + JP	one tag w/ NNtag
110 GeV	1.13 (7.0)	2.63 (16.2)	4.68 (28.9)
115 GeV	1.08 (8.2)	2.58 (20.0)	4.13 (31.4)
120 GeV	1.03 (10.0)	2.63 (25.7)	3.68 (36.0)
130 GeV	1.08 (17.2)	2.48 (39.7)	2.83 (45.3)
140 GeV	1.33 (43.3)	2.23 (72.7)	2.43 (79.2)
150 GeV	1.68 (142.8)	2.13 (181.2)	1.93 (164.1)

Table 13: This table shows observed upper limit using NN shape fit for each mass point and each tagging category. The values in parentheses mean upper limit normalized to SM expectation

10 Conclusions

We have presented the results of a search for the Standard Model Higgs boson via associated WH production and decay to $b\bar{b}$. This analysis is studied one SECVTX tagged events and two double btagged events. We find that for the dataset corresponding to integrated lumi-

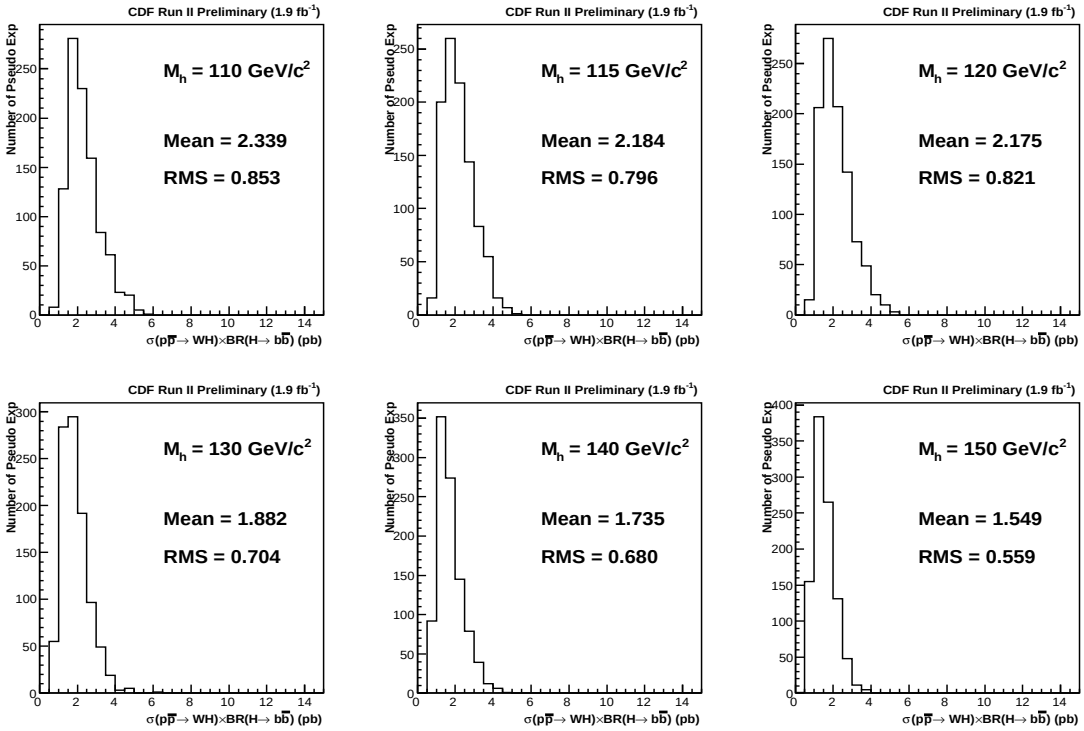

Figure 53: The results using NN output for one SECVTX tag plus Jet Probability tag with one thousand pseudo experiments for each Higgs mass. The results show 95% C.L. upper limit for each pseudo experiment.

Mass/b-tagging category	ST +ST & ST + JP	1tag & 2tag
110 GeV	1.08 (6.7)	1.33 (8.2)
115 GeV	1.03 (7.8)	1.18 (8.9)
120 GeV	0.98 (9.6)	1.13 (11.0)
130 GeV	1.08 (17.2)	1.08 (17.2)
140 GeV	1.18 (38.4)	1.18 (38.4)
150 GeV	1.48 (125.7)	1.23 (104.4)

Table 14: This table shows observed upper limit using NN shape fit for each mass point and each tagging category. The values in parentheses mean upper limit normalized to SM expectation

nosity of 1.9fb^{-1} , the observed data for each tagged events agrees with the SM background predictions within the systematic uncertainties. Therefore we set upper limit on the Higgs production cross section using 1tagged and 2tagged events. The observed limit using the neural network output distribution is $\sigma(p\bar{p} \rightarrow W^{\pm}H) \times BR(H \rightarrow b\bar{b})$ ranging from 1.3pb (for m_h = 110 GeV/c^2) to 1.2pb (for m_h = 150 GeV/c^2) at 95% confidence level.

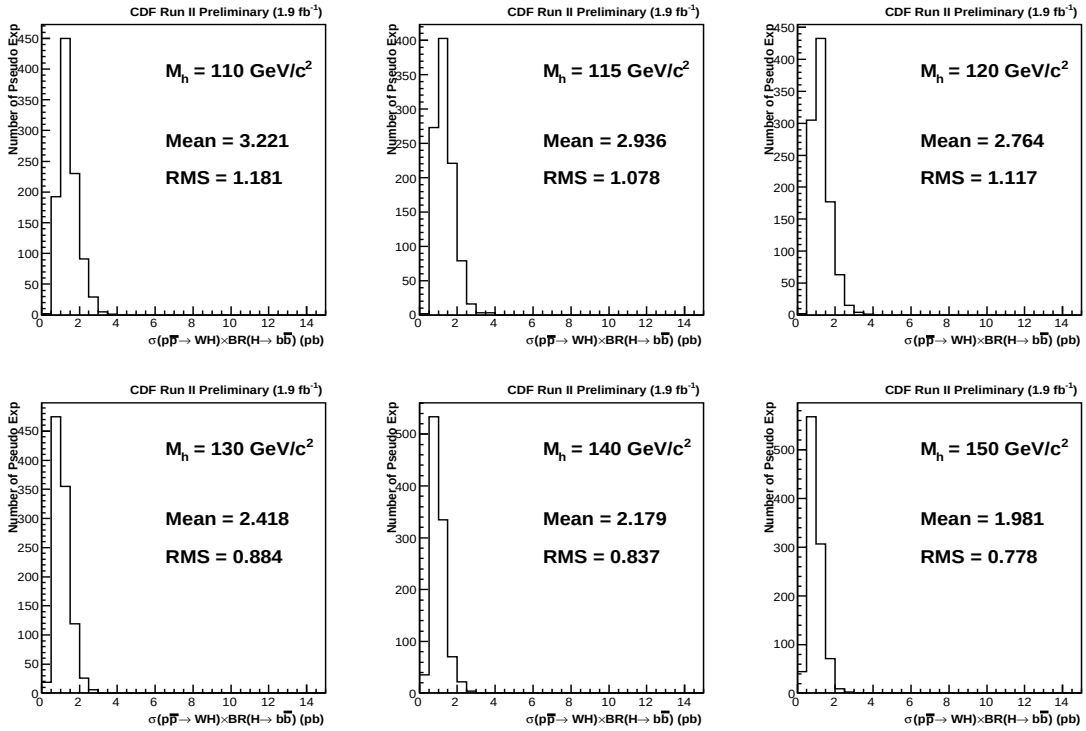

Figure 54: The results using NN output for the combination of ST+ST and ST+JP with one thousand pseudo experiments for each Higgs mass. The results show 95% C.L. upper limit for each pseudo experiment.

References

[1] Tev4LHC Higgs working gropu at http://maltoni.home.cern.ch/maltoni/TeV4LHC/SM.html

[2] http://www.physics.ucdavis.esu/ conway/research/higgs/higgs.html

[3] Y. Kusakabe it et al., "Search for Standard Model Higgs Boson Production in Association with $W^{\pm}$ Boson at CDF with $\int \mathcal{L}dt$ = 695 pb^{-1}, CDF Note 8194

[4] Y. Kusakabe it et al., "Search for Standard Model Higgs Boson Production in Association with a $W^{\pm}$ Boson at CDF with $\int \mathcal{L}dt$ = 1.0 fb^{-1}, CDF Note 8355

[5] H.Bachacou, P.Lujan, M.McFarlane, W.Yao, Advanced Heavy Flavor Tagging Using a Neural Network, CDF Note 7742

[6] http://ncdf70.fnal.gov:8001/PerfIDia/PerfIDia.html

[7] Han, Boisvert, "Trigger Efficiencies for the High Et Central Electron in the Gen6 data", CDF Note 8629

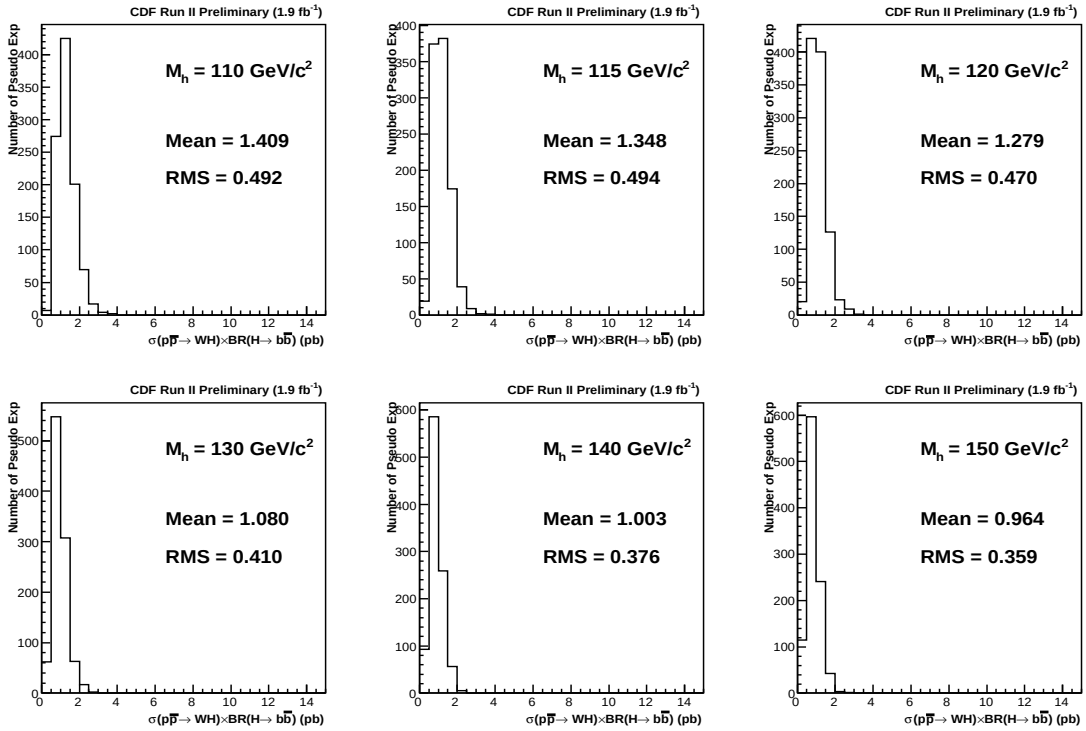

Figure 55: The results using NN output for the combination of 1tag and 2tag with one thousand pseudo experiments for each Higgs mass. The results show 95% C.L. upper limit for each pseudo experiment.

[8] Hare, Halkiadakis, Spreitzer, "Electron ID Efficiency and Scale Factors for Winter 2007 Analyses", CDF Note 8614

[9] Grundler, Lovas, Taffard, "High-Pt muons recommended cuts and efficiencies for Winter 2007", CDF Note 8618

[10] http://www-cdf.fnal.gov/internal/physics/joint_physics/index.html

[11] Grintein, Guimaraes da Costa, Shrman, "Electron-Method SecVtx Scale Factor for Winter 2007", CDF Note 8625

[12] Budd, S. et al., "Tight, Loose and Ultratight SECVTX Tag Rate Matrix with 1.2 fb^{-1} ", CDF Note 8519

[13] Grintein, Guimaraes da Costa, Shrman, "SecVtx Mistag Asymmetry for Winter 2007", CDF Note 8626

[14] Frankli, Grinstein, Guimaraes da Costa, Lannon, Schwarz, Sherman and Taffard, "Method 2 Backgrounds for 1.12/fb Lepton+Jets Analysis, CDF Note 8766

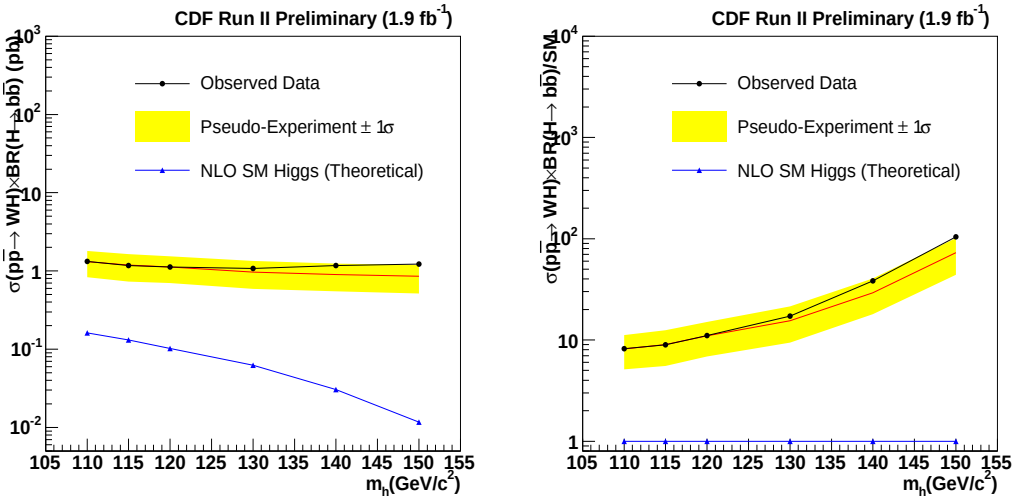

Figure 56: Observed limit calculated from NN shape. This plot shows double tight SECVTX and one tight SECVTX + jet probability combined results

[15] Franklin, Grinstein Sherman, "Measurement of the Top Pair Cross Section in Lepton+Jets in 1.12/fb, CDF Note 8768

[16] H. Bachacou, C. Feretti, J. Nielse, W.Yao, "Heavy Flavor contributions to the SECVTX-tagged W+Jets sample" CDF note 7007

[17] J. Efron et al., "Improved search for ZH to llbb in 1 fb-1", CDF Note 8704.

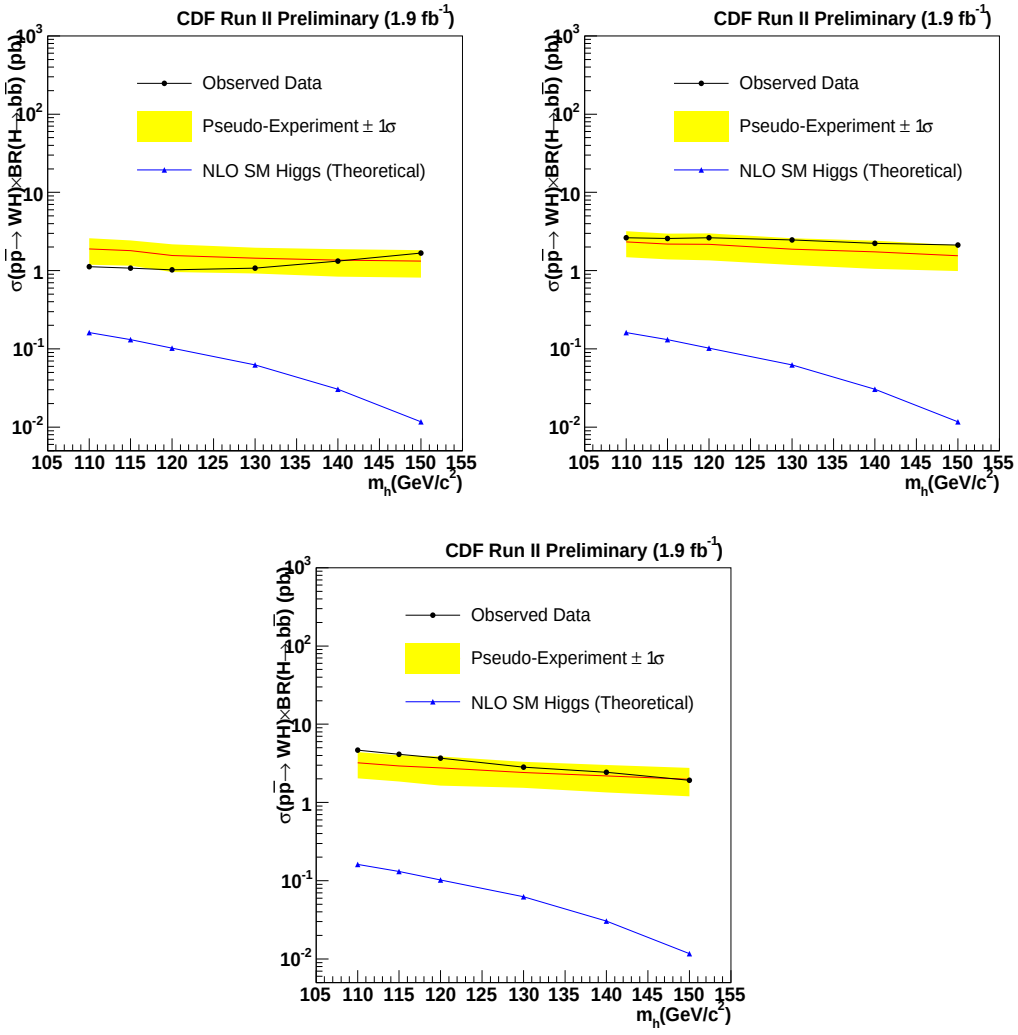

Figure 57: Observed limit calculated from NN shape for each tagging category